NAVAL POSTGRADUATE SCHOOL
Monterey, California

THESIS

DESIGN OF A STABILIZED, DC-POWERED
ANALOG LASER DIODE DRIVER

by

John Joseph Bradunas

September 1990

Thesis Advisor: John P. Powers

REPORT DOCUMENTATION PAGE

Form Approved OMB No 0704-0188

1a REPORT SECURITY CLASSIFICATION: UNCLASSIFIED	1b RESTRICTIVE MARKINGS
2a SECURITY CLASSIFICATION AUTHORITY	3 DISTRIBUTION / AVAILABILITY OF REPORT: Approved for public release; distribution is unlimited
2b DECLASSIFICATION / DOWNGRADING SCHEDULE	
4 PERFORMING ORGANIZATION REPORT NUMBER(S)	5 MONITORING ORGANIZATION REPORT NUMBER(S)
6a NAME OF PERFORMING ORGANIZATION: Naval Postgraduate School; 6b OFFICE SYMBOL (If applicable): EC	7a NAME OF MONITORING ORGANIZATION: Naval Postgraduate School
6c ADDRESS (City, State, and ZIP Code)	7b ADDRESS (City, State, and ZIP Code)
8a NAME OF FUNDING / SPONSORING ORGANIZATION; 8b OFFICE SYMBOL (If applicable)	9 PROCUREMENT INSTRUMENT IDENTIFICATION NUMBER
8c ADDRESS (City, State, and ZIP Code)	10 SOURCE OF FUNDING NUMBERS: PROGRAM ELEMENT NO; PROJECT NO; TASK NO; WORK UNIT ACCESSION NO

11 TITLE (Include Security Classification)
DESIGN OF A STABILIZED, DC-POWERED LASER DIODE DRIVER

12 PERSONAL AUTHOR(S)
BRADUNAS, John J.

13a TYPE OF REPORT	13b TIME COVERED	14 DATE OF REPORT (Year, Month, Day)	15 PAGE COUNT
Master's Thesis	FROM _____ TO _____	September 1990	

16 SUPPLEMENTARY NOTATION The views expressed in this thesis are those of the author and do not reflect the official policy or position of the Department of Defense or the US Government.

17 COSATI CODES			18 SUBJECT TERMS (Continue on reverse if necessary and identify by block number)
FIELD	GROUP	SUB-GROUP	semiconductor laser diode; thermoelectric cooling; laser diode driver; intensity modulation

19 ABSTRACT (Continue on reverse if necessary and identify by block number)

This thesis presents the design, implementation and evaluation of a de-powered, stabilized-output laser diode drive unit for use in an analog fiber-optic communication transmitter. The driver circuits provide for a stable temperature-controlled operating environment by monitoring the thermistor in the laser diode module and by controlling the current to the module's integral thermoelectric cooler. Output optical power is maintained at desired bias and peak-to-peak levels by processing the signal from the monitor photodiode and amplifying (if necessary) the ac and dc drive units. These efforts offset the degradation of the laser diode's capabilities due to heat and age.

20 DISTRIBUTION / AVAILABILITY OF ABSTRACT: ☒ UNCLASSIFIED/UNLIMITED ☐ SAME AS RPT ☐ DTIC USERS	21 ABSTRACT SECURITY CLASSIFICATION: UNCLASSIFIED
22a NAME OF RESPONSIBLE INDIVIDUAL: POWERS, John P.	22b TELEPHONE (Include Area Code): 408-646-2679; 22c OFFICE SYMBOL: EC/Po

DD Form 1473, JUN 86 *Previous editions are obsolete*

Approved for public release; distribution is unlimited.

Design of a Stabilized, DC-Powered
Analog Laser Diode Driver

by

John J. Bradunas
Major, United States Marine Corps
B.S., Cornell University

Submitted in partial fulfillment
of the requirements for the degree of

MASTER OF SCIENCE IN ELECTRICAL ENGINEERING

from the

NAVAL POSTGRADUATE SCHOOL
September 1990

Author: 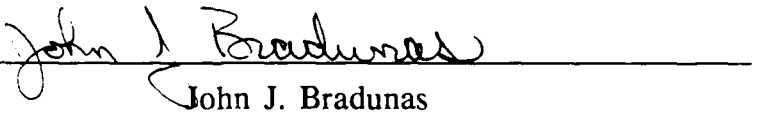
John J. Bradunas

Approved by: 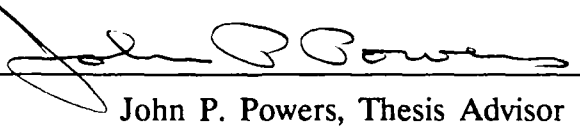
John P. Powers, Thesis Advisor

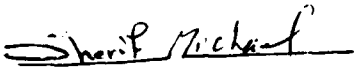
Sherif Michael, Second Reader

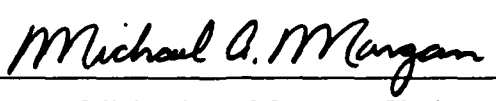
Michael A. Morgan, Chairman
Department of Electrical and Computer Engineering

ABSTRACT

This thesis presents the design, implementation and evaluation of a dc-powered, stabilized-output laser diode drive unit for use in an analog fiber-optic communication transmitter. The driver circuits provide for a stable temperature-controlled operating environment by monitoring the thermistor in the laser diode module and by controlling the current to the module's integral thermoelectric cooler. Output optical power is maintained at desired bias and peak-to-peak levels by processing the signal from the laser diode's monitor photodiode and amplifying (if necessary) the ac and dc drive currents. These efforts offset the degradation of the laser diode's capabilities due to heat and age.

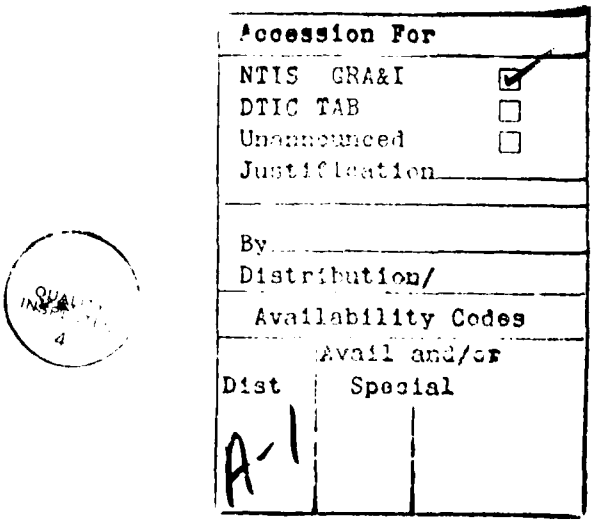

TABLE OF CONTENTS

LIST OF TABLES

LIST OF FIGURES

I. INTRODUCTION

A. BACKGROUND

This thesis is a continuation of ongoing research being conducted at the Naval Postgraduate School involving the development of fiber-optic communication links for use in hostile environments. The particular goal of this research effort was to design, implement and evaluate a stabilized, dc-powered laser diode (LD) drive unit which can be used to transmit analog signals over fiber-optic cables.

The light output of a laser diode can be directly modulated by varying the amount of applied current. The results of this method can be seen in the typical output versus drive current curve shown in Fig. 1.1. Such a modulation technique has the advantage of simplicity and the potential for high-speed operation. However, the physical process of producing coherent light creates thermal and aging problems which directly affect the operational stability of the laser diode, possibly resulting in an undesirable optical output or even damage to the module itself. Consequently, a network was created which maintains a stable operating environment within the module and which can electrically modify the input to the laser diode in order to achieve desired optical levels.

B. THESIS OBJECTIVES

The major design requirements for the driver mechanism built during this thesis effort were:

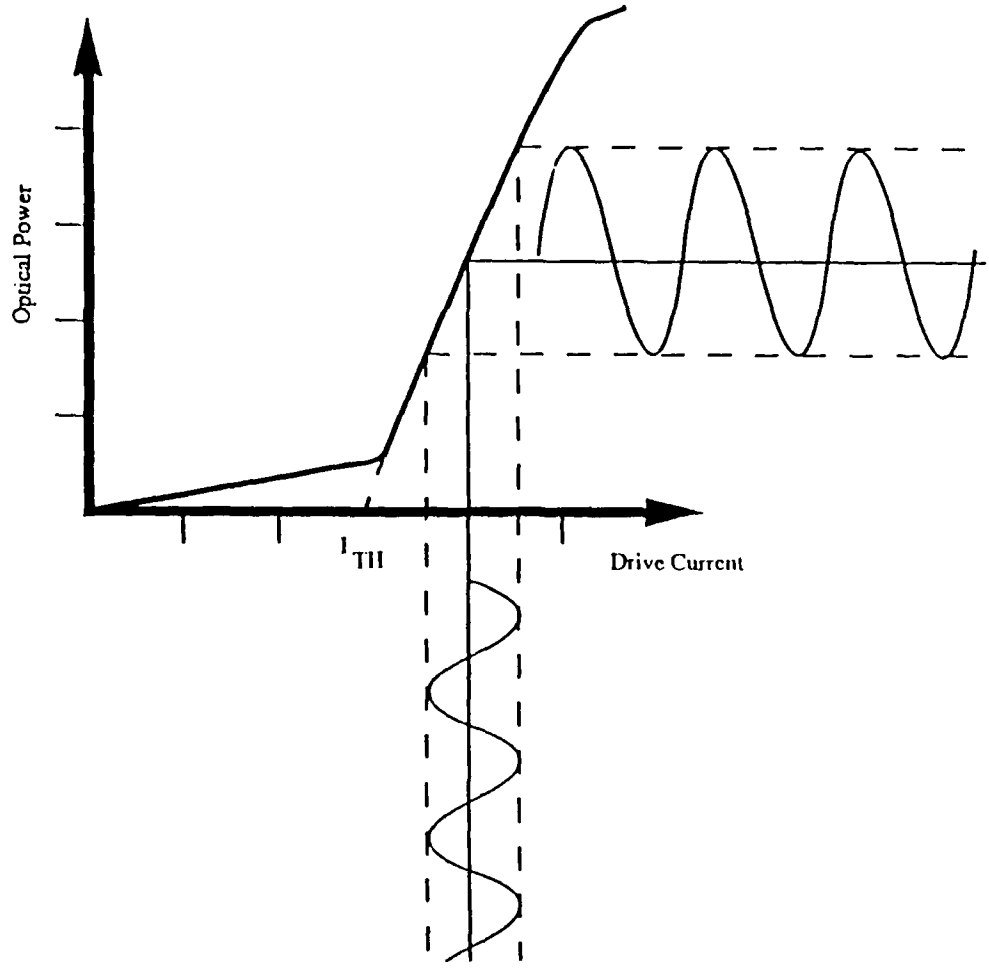

Figure 1.1. Direct Modulation of a Laser Diode (after Ref. 1).

- to modulate a laser diode with an analog signal at or near 100 kHz,
- to use only low-power voltage sources,
- to be capable of driving various types of laser diodes and light-emitting diodes (LEDs),
- to implement a network to operate a thermoelectric cooler and maintain a stable, adjustable operating temperature,
- to maintain a stabilized optical output with the capability of adjusting the desired bias and peak power levels and
- to provide drive current limiting and surge current protection for the laser diode.

C. SYSTEM DESIGN OVERVIEW

Figure 1.2 is a simplified functional schematic of a laser transmitter. Those items enclosed by the dashed lines are normally included in a single laser diode module. The two major components of the stabilization mechanism, the cooling system and bias network, are discussed in detail in this thesis. Chapter II discusses the operation of a laser diode, highlighting the specific problems which affected the network design. Chapter III describes the temperature stabilization circuit, specifically addressing the Peltier effect and the technique of thermoelectric cooling. Chapter IV presents the network used to maintain the bias point and the peak optical output power levels from the laser diode; this involves the extensive use of high-speed operational amplifiers (op-amps) in signal-processing circuits. Both stabilization networks are tested and evaluated in Chapter V by using the driver to transmit various waveforms via a fiber optic cable. Finally, Chapter VI contains concluding remarks and recommendations for areas of further research.

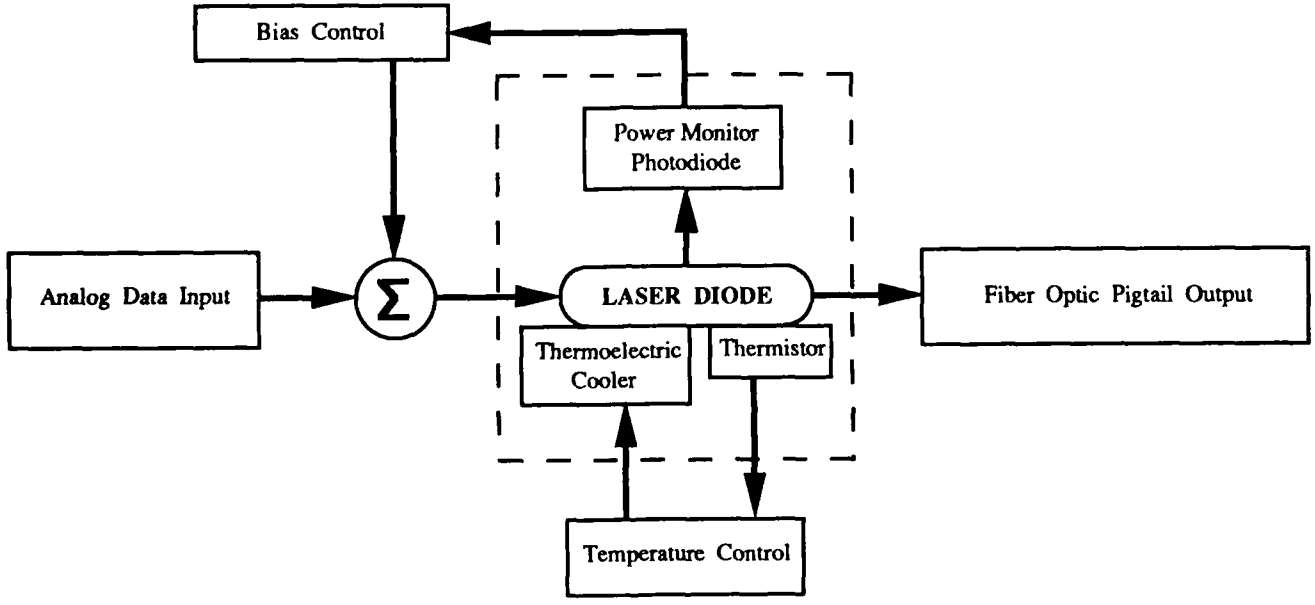

Figure 1.2. Functional Schematic of a Laser Transmitter.

II. LASER DIODE PHYSICS

A. RADIATIVE RECOMBINATION

Energy level diagrams for semiconductor materials used in lasing are not as sharp and distinct as those of other lasing media such as ruby or neon. Atoms in n- and p-type materials are packed so closely together that separate energy levels are difficult to distinguish; therefore the levels are grouped into bands. Although energy distributions within the semiconductors can still be represented by the Einstein relations for absorption and emission, optical transitions are between bands vice discrete energy levels.

Electrons with the highest energy (i.e., those in the outermost ring around their nucleus) occupy the conduction band. These electrons have enough energy to carry an electrical current and consequently move easily through the semiconductor material. The next highest energy state is the valence band; at these levels, electrons are still tied to their parent nucleus and cannot carry a current, however they can be excited and moved to the conduction band. In order for an electron to transition to the higher band, it must receive sufficient energy to exceed the gap potential between the valence and conduction bands. In addition to the absorption of this energy difference, the probability of such a transition must also be sufficiently high. If both of these conditions are met, the basic building blocks for the creation of light exist, an excited electron in a high-energy band and a matching positive carrier (i.e., hole) ready for recombination.

At the junction of an n- and p-type semiconductor, a thin depletion region is formed by the recombination of these carriers. As shown in Fig. 2.1a, this region forms a barrier (or bandgap) potential between the n- and p-type materials. With no voltage applied across the semiconductor, the barrier prevents the interdiffusion of charge carriers (the holes and electrons) from their respective regions. When a forward voltage is applied as in Fig. 2.1b, the barrier is reduced and carriers are "injected" into the junction region--hence, the term injection laser [Ref. 1:p. 12].

Equilibrium is achieved via two types of recombination. Nonradiative recombinations result in vibrations in the materials crystal lattice, producing heat [Ref. 2:p. 249]. However, if the recombination is radiative, a photon is emitted; the amount of energy in the released photon approximately equals E_g, the bandgap potential between the valence and conduction bands of the material. The wavelength of the light emitted is determined by

$$\lambda \approx \frac{h c}{E_g} \tag{2.1}$$

where h is Planck's constant (6.63×10^{-34} J-s) and c is the speed of light in a vacuum (3.00×10^{8} m-s^{-1}). This phenomenon of light production via induced carrier recombination at the junction of semiconductor material is called "electroluminescence." [Ref. 1:p. 11]

Up to this point, discussion of the production of light has not distinguished between the types of emissions that could result from radiative recombinations. As noted, the application of a forward voltage across a semiconductor, inducing

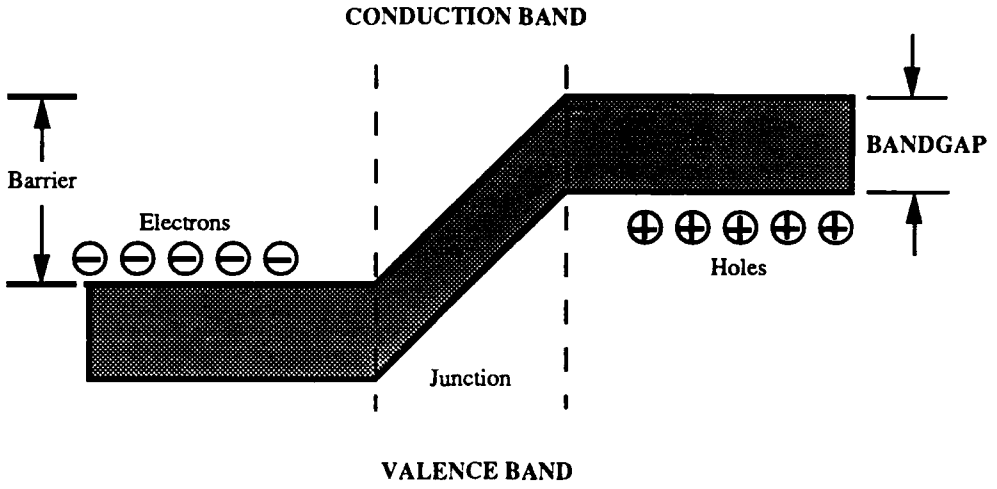

a) No Voltage Applied

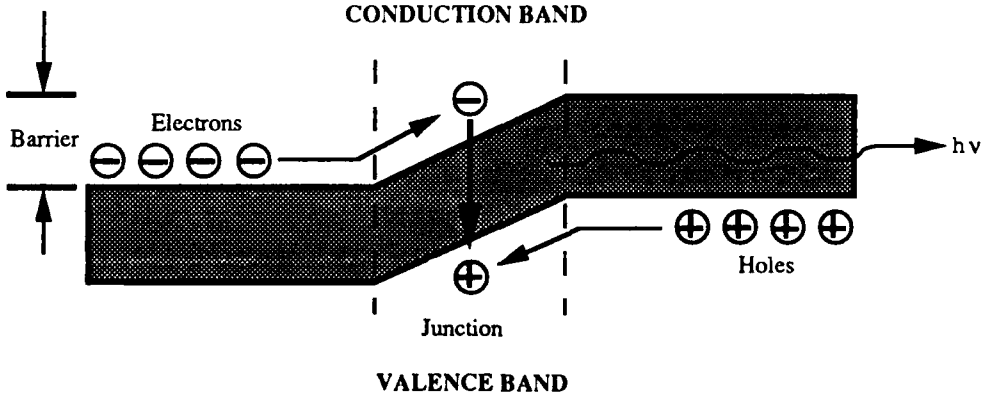

b) Forward Voltage Applied

Figure 2.1. Energy Level Diagram of a pn-Junction (after Ref. 1).

a current through the structure, can lead to the release of photons. If this current is kept below a certain critical value, called the lasing threshold (or I_{TH}), the semiconductor device emits noncoherent light spontaneously and randomly (i.e., it functions as a light emitting diode). However, when sufficient current is applied to the junction, more electrons are moved to an excited state and a population inversion is achieved. At that time a randomly emitted photon from a recombination can act to *stimulate* another recombination and emission, which can emit another photon, and so on. This chain reaction amplifies the light as it passes through the material, producing a coherent output (hence the acronym LASER--Light Amplification by Stimulated Emission of Radiation). Semiconductor devices which can act as lasers are known as semiconductor laser diodes, or simply laser diodes. Figure 2.2 shows a typical power versus current relationship in a laser diode; the effect of a drive current exceeding I_{TH} is apparent by the increased slope of the output curve.

B. LASING CAVITIES

In order to sustain this amplification, opposite faces of the semiconductor structure are cleaved along crystalline planes to create parallel reflective surfaces. This in effect forms an optical cavity similar to a Fabry-Perot interferometer. The end mirrors created by the cleaving reflect some of the photons back into the active light-producing region surrounding the pn-junction. The feedback creates an oscillatory wave of light along the junction which equals cavity losses and helps to sustain the stimulated emissions. The reflectivity at the cleaved surface can be

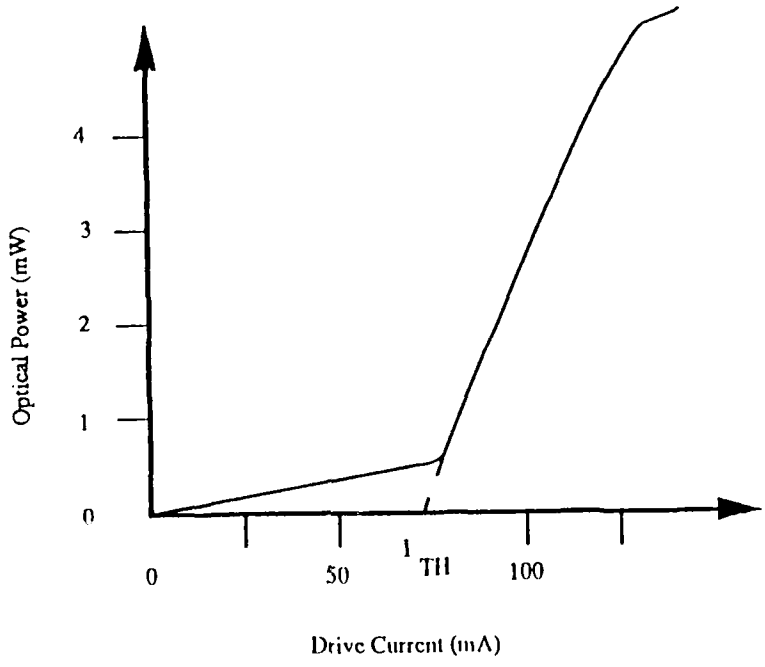

Figure 2.2. Transfer Function of a Laser Diode (after Ref. 2).

estimated by the Fresnel formula for normal incidence

$$R = \left[\frac{n_1 - n_2}{n_1 + n_2}\right]^2 \tag{2.2}$$

where n_1 and n_2 are the refractive indices of the cleaved material and surrounding medium (usually air). Reflectivities of 30% can be produced by this mechanical technique, a level suitable for low power operation [Ref. 3:p. 14].

Higher reflectivities, and consequent increased emission efficiencies, can be achieved by adding reflective surface to each face. Pure metal coatings (such as gold) are troublesome since the applied layer is easily damaged during laser diode fabrication and degrades over time at room temperature [Ref. 3:p. 28]. One alternative that is proving successful is to deposit quarter-wavelength anti-reflective layers of suitable dielectrics (such as SiO and Al_2O_3) on the end faces and then

applying a highly reflective silver layer onto the dielectric. Although there remains a design problem to ensure only slight degradation in performance over time, reflectivities approaching 98% have been achieved [Ref. 4:p. 96].

C. OUTPUT CHARACTERISTICS

While Eq. 2.1 shows the relation between the wavelength of the emitted light and the material-dependent bandgap energy E_g, dopants in the n- and p-type materials can be used to vary the wavelength of the emitted light. For example, the wavelength of light emitted from a GaAs semiconductor laser diode can range between 0.85 μm and 0.95 μm depending on the doping concentrations [Ref. 2:p. 256]. Typical n-material dopants including silicon, tin (Sn), tellurium (Te) and germanium, while zinc (Zn), tin, tellurium and germanium are used to dope p-type regions [Ref. 5:p. 236].

Another major factor in determining output wavelength, and one of the major drawbacks in the use of laser diodes, is the strong dependence of the lasing threshold current on temperature. Studies have shown that as the junction temperature increases, the bandgap energy decreases, in a typical lightly-doped active region, at a rate approximately equal to 0.5 meV-K^{-1} [Ref. 3:p. 36]. This energy shift also increases the output wavelength by 0.3 to 0.5 nm-K^{-1} due to the near-linear relation of E_g and λ, as demonstrated in Eq. 2.1 [Ref. 6]. However, compounds with high bandgap energies are less sensitive to increases in temperature since they can maintain carrier confinement over a wider temperature range [Ref. 3:p. 20].

The increase in junction temperature also forces an increase in the threshold current necessary to maintain the diode in the lasing region of the power-current spectrum. Figure 2.3 is an example of the output variations caused by junction heating. It has been shown experimentally that the threshold current of most laser diodes changes exponentially with junction temperature, i.e.,

$$\frac{I_{TH_1}}{I_{TH_2}} = \exp\left[\frac{T_1 - T_2}{T_0}\right] \tag{2.3}$$

where T_1 and T_2 are the temperatures in the active region and T_o is a material-dependent temperature constant [Refs. 3:p. 20 and 2:p. 281]. This exponential relationship can be approximated over small regions by a linear rate of change of about 1.5%-K^{-1} [Ref. 7:p. 140]. In other words, at a constant current, the radiated power would be significantly reduced as the temperature rises; the shifting output curve may allow the device to leave the lasing region and revert to LED-type radiation or may drive the diode into a non-linear output region (see Fig. 2.3).

D. LASER DIODE MATERIALS

Unfortunately, not all semiconductor materials are useful as lasing media. When the first high-efficiency light generation from a pn-junction was reported by RCA Laboratories in 1962, it was recognized that the (then) most common semiconductor materials--silicon (Si) and germanium (Ge)--were not suitable as optical sources. It was discovered that Si and Ge have a low probability for radiative recombination compared to nonradiative emissions. This was due to the

fact that Si and Ge, both Group IV elements in the periodic table, are indirect bandgap materials. [Ref. 1:p. 15]

In the junction of direct bandgap (Groups III and V) semiconductors, opposing charge carriers in different bands have the same value of crystal

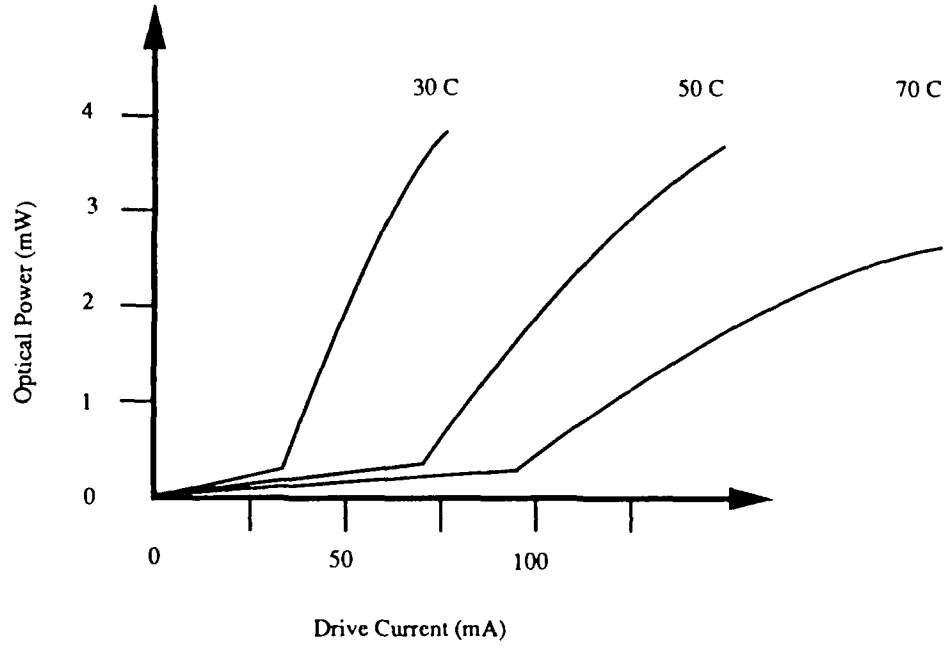

Figure 2.3. Temperature Dependence of a Laser Diode (after Ref. 2).

momentum; i.e., the energy maximum of a hole in the valence band is approximately equal to the energy minimum of an electron in the conduction band. Therefore, at recombination, electron momentum is nearly constant and the energy released (E_g) is nearly all in the optical spectrum.

However, in indirect bandgap materials, these minimum/maximum energy levels do not correspond and a third particle of energy (a phonon) is needed to equate the two energy levels and to produce a photon. This three-particle process

has a much lower probability of occurring than a two-particle direct bandgap recombination, therefore Si and Ge semiconductors are much less likely to produce light than combinations of gallium (Ga), arsenide (As), antimide (Sb), indium (In) or phosphide (P) compounds, all of which are Group III or V elements. A detailed discussion of material suitability for the production of coherent light is discussed in Refs. 3:p. 10 and 2:pp. 250-252.

E. LASER DIODE DESIGNS

1. Single Heterostructures

The discussion thus far has described the capabilities and operating requirements for a laser diode constructed of a single alloy doped to form n- and p-type regions. Such homostructures have inherent limitations which prevent high efficiencies in producing optical power:

- charge carriers diffuse within the pn-junction active region due to Coulomb repulsion, reducing the carrier density which reduces the probability of radiative recombination and
- the light produced in the active region tends to spread as it propagates through the device, causing a rapid expansion of the optical wavefront beyond the active region where it no longer contributes to the oscillation process. [Ref. 8:p. 268]

Hence, to increase the efficiency of the laser diode, a technique is needed to reduce the effects of these problems (i.e., somehow the diode must be modified to confine both the charge carriers and the light wave to a smaller region).

In 1968, Bell and RCA Laboratories came up with a possible solution to these problems, a heterostructure laser diode was constructed [Ref. 1:p. 28]. A junction was created by matching two dissimilar materials which have close to the same atomic spacings. GaAs was used form the n-type region and AlGaAs the p-type. This single heterostructure device displayed two improvements over earlier homostructure diodes:

- The stimulated electron carriers were confined to a thin region adjacent to the junction thereby keeping carrier density high in a small area and allowing radiative recombinations to occur in a controlled region of the device.
- Since AlGaAs has a lower index of refraction than GaAs, most of the light produced in the junction was prevented from escaping into the light-absorbing p-type material and was reflected back into the active region around the junction. [Ref. 1:p. 28]

The heterostructure provides a dielectric cavity which acts as an optical waveguide. It is precisely this fact which led to the large reduction in threshold current in semiconductors at room temperature and made the laser diode practical as a coherent light source. Heterostructures reduced the current density requirements in the active region to approximately 100 A-cm^{-2} in order to induce lasing; homostructure diodes required densities of 50,000 to 100,000 A-cm^{-2}. [Ref. 3:p. 10]

2. Double Heterostructures

The success of single heterostructure devices inevitably led to the development of double heterostructure diodes. Figure 2.4 is a representative example of the improved system. Upon a substrate of n-type GaAs is grown

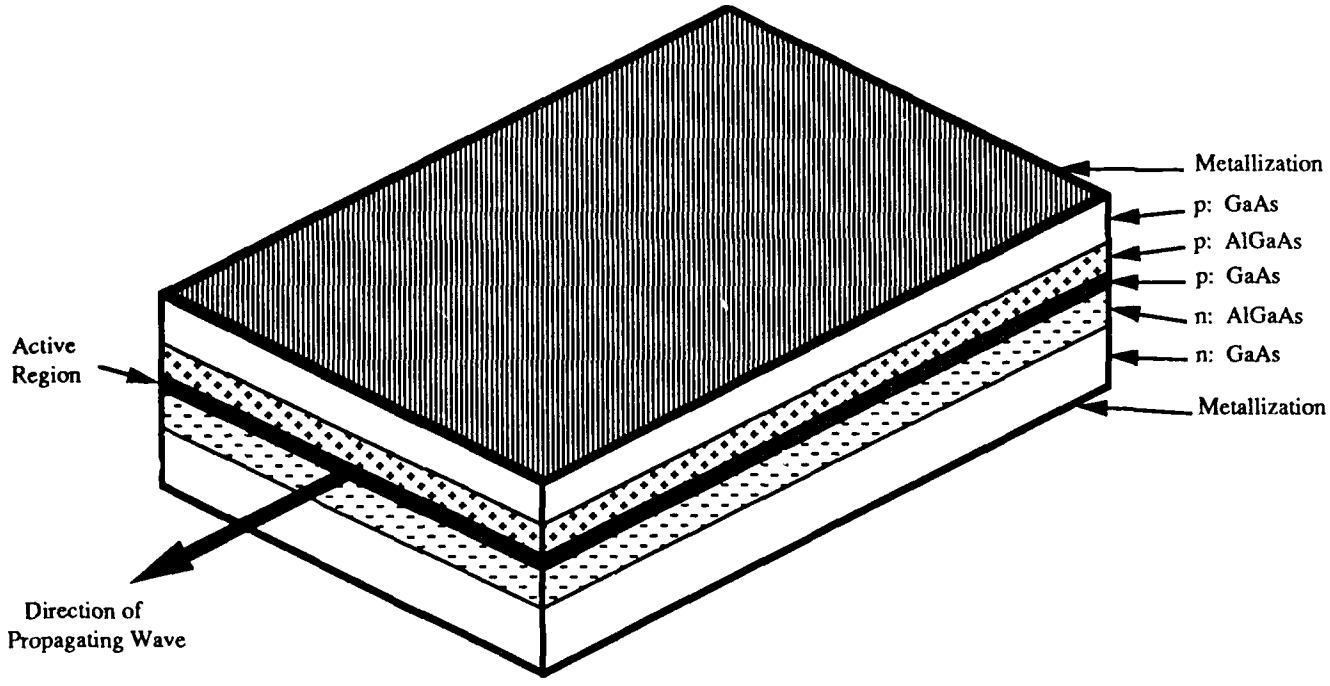

Figure 2.4. Double Heterostructure Laser Diode (after Ref. 1).

successive layers of n-type AlGaAs, p-type GaAs, p-type AlGaAs and finally p-type GaAs (used solely to facilitate the attachment of electrical contacts). The small active region of p-type GaAs is surrounded by the AlGaAs alloy which has, as mentioned before, a lower index of refraction. Therefore, light is reflected back at the junction boundary above and below the active region as the wave oscillates through the device.

The energy level diagram of Figure 2.5 demonstrates how an InGaAsP/InP double heterostructure diode confines charge carriers to the active region. The applied forward voltage allows the carriers to easily enter the active region from their respective materials. However, the energy level difference between the active region and its adjacent layers forms a barrier potential which keeps the electrons and holes within the small area. The current density is consequently kept high which increases the probability of a *stimulated emission* and therefore raises the power output and overall efficiency of the system to 10%, nearly twenty times that of a homostructure diode. [Ref. 1:pp. 29-33]

As explained above and as can be seen in Figs. 2.4 and 2.5, double heterostructures limit the longitudinal and transverse power distributions within the diode, but provide little restrictions on lateral losses out the side of the active region. Although the use of mirrors or cleaving may improve these losses, there is a better way to completely confine the active region. By etching a narrow mesa stripe in a double heterostructure semiconductor and then burying the combination in a high resistivity, lattice-matched n-type material (with a higher bandgap energy and lower index of refraction), the active region would be strictly confined on all

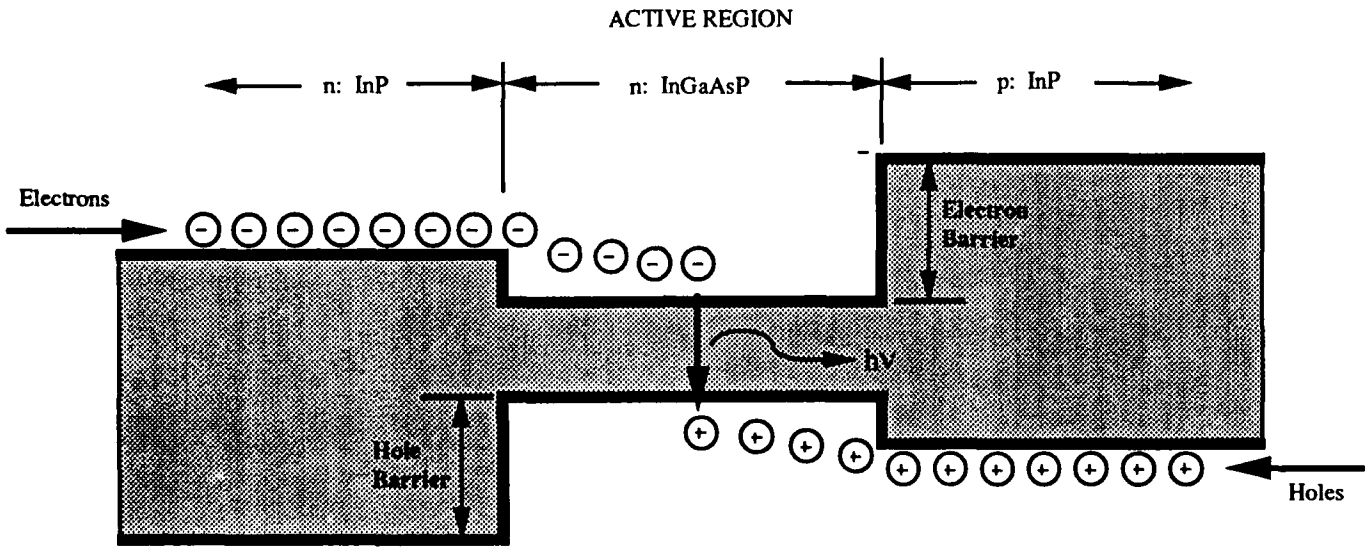

Figure 2.5. Energy Level Diagram of a Double Heterostructure Laser Diode (after Ref. 7).

four longitudinal surfaces. Consequently, both the charge carriers and light wave would be contained within an extremely small area. [Ref. 2:p. 273]

Figure 2.6 is an end view of such a buried double heterostructure laser diode. The active region is the n-type InGaAsP material surrounded by higher bandgap energy and lower index of refraction materials, keeping most of the charge carriers and the optical output in the small area. This reduction in the size of the active region allows for a further reduction in the necessary threshold current to values less than 20 mA. It is also easier to produce a reasonably defect-free active region because of its relatively small size. In addition, the thermal resistance in this area is generally reduced since more of the heat produced by nonradiative recombination can be conducted into the large surrounding inactive semiconductor regions. The surrounding materials also protect this critical region from external contaminants along its major dimensions, a situation important for long-term stable operation. [Ref. 3:p. 23]

Well-designed buried double heterostructure diodes can produce a single-lobe Gaussian-shaped elliptical beam output; this is a single spatial mode device which is considered essential for modern fiber optic communication [Ref. 9:p. 163]. Such diodes have been tested with modulation bandwidths of 2 GHz; attached to a single-mode, step-index fiber, a transmitter sent information at a rate of 800 Mbps over 60 km without the use of electro-optic repeaters [Refs. 2:p. 273 and 10:p. 285].

The buried double heterostructure semiconductor is an example of an index-guided laser diode. Similar device types include buried crescent (BC),

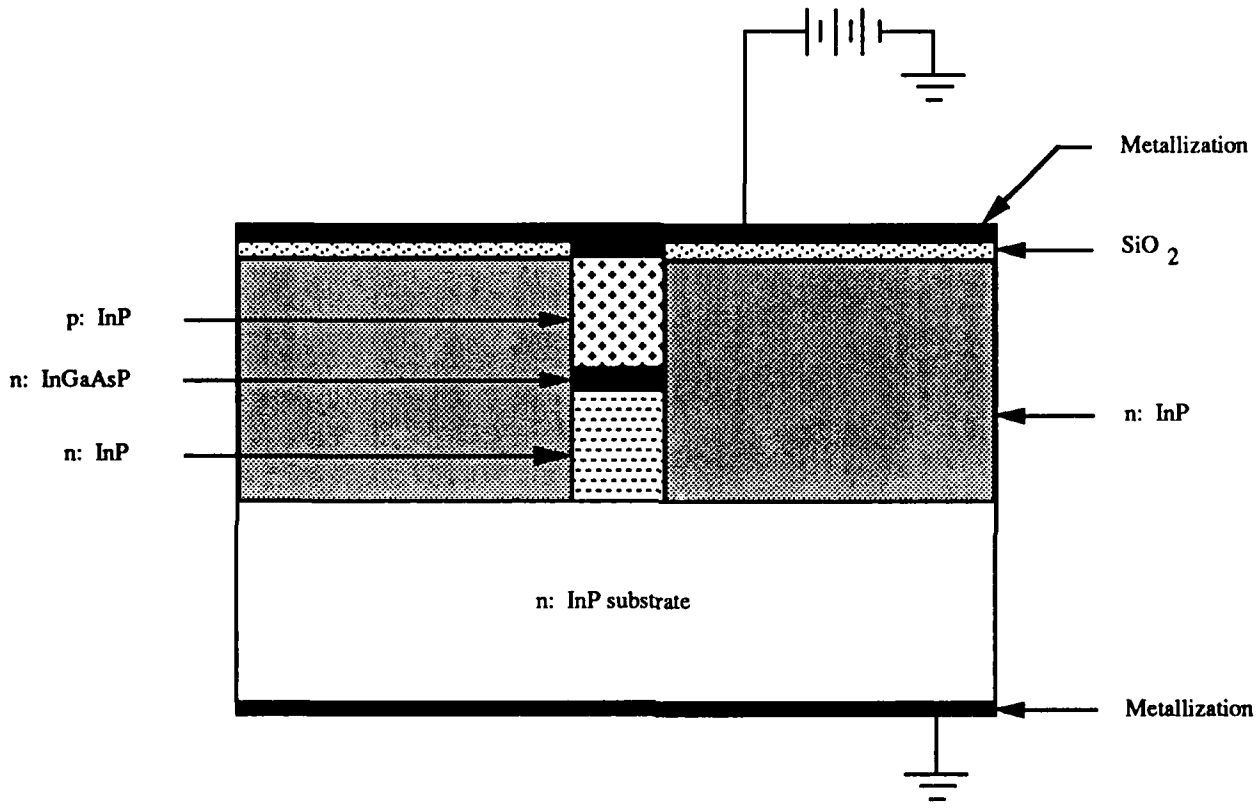

Figure 2.6. End View of a Buried Heterostructure InGaAsP/InP Laser Diode (after Refs. 2 and 7).

transverse junction stripe (TJS) and channel substrate planar (CSP) systems. The aforementioned performance improvements can also be achieved from a second family of double heterostructures. Classified as gain-guided devices, they create an optical waveguide and carrier confinement region not by the variation of refractive indices, but by the optical power gain introduced only by the injected charge carriers in the narrow stripe active region [Ref. 11:p. 191]. Examples of this type of laser diode include oxide stripe, diffused stripe, proton bombardment stripe and phase-locked array structures [Ref. 9:p. 162].

Gain-guided devices can achieve a high total output power, generally produce less noise in communication networks and are less susceptible to saturation via optical feedback [Ref. 12:p. 58]. However, index-guided laser diodes (such as the buried double heterostructure) have several distinct advantages:

- a sharper power versus current "knee" at the threshold current value,
- less spontaneous emission below threshold, allowing for a more efficient "on-off keying" communication scheme,
- a peak output power exceeding 10 mW in a single spatial mode,
- little or no astigmatism of the output wavefront (i.e., the beam appears to originate from the same location in both the horizontal and vertical planes allowing for easier coupling to a lens or fiber) and
- a very stable far-field pattern with respect to time, ensuring a relatively constant high-efficiency coupling into fibers with low numerical apertures, throughout the system lifetime. [Refs. 10:p. 291 and 13:p. 371]

F. RELIABILITY

Early laser diodes experienced extremely short lifetimes--1 to 100 hours--however, current crystal growth techniques and power systems have improved so that 50,000 hours of continuous operation are not uncommon [Ref. 14:p. 212]. Unfortunately, system reliability will always be affected by two major forms of degradation, gradual and catastrophic.

Gradual degradation can be caused by the formation of nonradiative recombination centers in the active regions. Under microscopic examination, these flaws appear as dark lines near the pn-junction and reduce the light-producing efficiency of the diode [Ref. 15:p. 290]. Another problem is the slow decay of the reflectivity of the end mirrors, possibly due to operation at excessive power levels. Joule heating, resulting from high current densities, can increase the thermal and electrical resistance of the metal contacts. As a general rule of thumb, increasing junction temperature by 10 C halves the expected mean-time-to-failure [Ref. 9:p. 167]. These three conditions may force an increase in the required threshold current I_{TH} and a decrease in the internal quantum efficiency, both of which lead to shorter diode lifetimes.

Gradual degradation typically occurs in three stages:

- a sudden decrease in operating efficiency with only minor changes in lasing properties (e.g., output power or wavelength),
- dark lines begin to appear in the emission pattern and
- the near-field pattern quickly develops "dark spots" accompanied by a rapid decrease in power output, even at stable (room) temperatures. [Ref. 3:p. 54]

Although gradual degradation is laser diodes cannot be eliminated, several techniques can been used to extend a structure's lifetime:

- improved material selection and precise crystal growth,
- improved fabrication techniques for the hardened reflective surfaces,
- better bonding of metallization layers on semiconductor materials and
- heat sinking of the substrate to lower the temperature of the active region.

Catastrophic degradation, as the name implies, is a sudden and (usually) unexpected failure of the laser diode system. Typically, the mirror facets are physically damaged, terminating any oscillation and output. The damage is usually the result of high input currents which produce excessive output power levels and acoustical shock waves in the active region which crack or melt the mirrors. Such a situation reduces the output power to zero almost immediately. Care must also be taken to ensure power-on/off current spikes and random transients are filtered to avoid temporary surges which exceed design input thresholds. However, by carefully monitoring the bias and modulation currents, this type of fatal damage can be avoided. [Ref. 9:p. 165]

G. CHOICE OF SOURCE

Although the laser driver design developed in this thesis can easily be adapted for use with a wide range of laser diodes, for purposes of clarity it will be convenient to choose a single representative device to aid in system development. Since this design was to power a light source in a fiber-optic

communication network, the device which best suits this application would be a logical choice as a "typical" laser diode.

Studies have shown that semiconductors which operate at long wavelengths (at or greater than 1300 nm) have several advantages for use in optical systems. Transmission losses with these sources are typically low, and modulation bandwidths can exceed 1 GHz [Ref. 12:p. 57]. In typical silica-based fibers, absorption mechanisms restrict wavelengths to less than 1600 nm and OH absorption is dominant at 1400 nm [Ref. 10:p. 285]. However losses with a 1300 nm source have been shown to be 0.35 $dB\text{-}km^{-1}$ compared to 1.81 $dB\text{-}km^{-1}$ for 850 nm and 0.40 $dB\text{-}km^{-1}$ for 1380 nm light [Ref. 16]. Consequently, a 1300 nm laser diode is a good choice for use in long-haul, high-bandwidth data transfer systems.

The previous sections have demonstrated the superior design of a buried heterostructure diode in terms of stability and efficiency. After several experiments with various combinations of elements in building a buried heterostructure, the quaternary alloy InGaAsP, grown on an InP substrate, proved very favorable for both sources and detectors operating at a wavelength of 1300 nm. Specifically, the chemical compositions under study [in Ref. 3:p. 14] were

$$In_xGa_{1-x}As_yP_{1-y} \tag{2.4}$$

where x and y indicated mole fractions in the alloy and were related by

$$y \approx 2.16\,(1 - x) \tag{2.5}$$

By varying the value of x (and therefore y), the output wavelength of the laser diode can be adjusted.

However, this combination does have a potential problem area; its extreme sensitivity to temperature can result in a large and rapidly rising nonradiative recombination current in the active region [Ref. 2:p. 282]. A slight increase in junction heating could drastically increase I_{TH} and produce a wide swing in spectral emissions. For example, using Eq. 2.3 and a typical value of 60 C for T_o in InGaAsP semiconductors, a 60 C temperature increase in the active region would increase I_{TH} by a factor of 2.7 [Ref. 9:p. 165]. With a InGaAsP laser diode, this temperature difference can force a shift in peak wavelength of 0.1 nm for every degree C increase [Ref. 9:p. 165].

Emphasis must therefore be placed on temperature stability during the design process; this is required not just to maintain a specific I_{TH} and output wavelength but also, as mentioned earlier, to reduce the likelihood of a catastrophic failure and to delay the effects of gradual degradation (e.g., cooling can be increased as a diode ages so that I_{TH} can be kept relatively constant over a device's lifetime).

The source used in this design process was the Lasertron QLM-1300-SM-BH, a 1300 nm GaInAsP/InP single-mode, buried-heterostructure laser module containing a thermoelectric cooler, thermistor and GaInAs/InP monitor photodiode. A single-mode fiber pigtail is coupled to the laser and provides

minimum optical feedback and good coupling efficiency. Table 1 lists pertinent features of this source.

TABLE 1. QLM-1300-SM-BH LASER DIODE [Ref. 17]

Continuous Wave (CW) rated output power		1.00 mW
Threshold current		36.0 mA
Peak wavelength (at 0.5 mW CW output power at 25 C)		1290 nm
Supply current at rated output power		45.0 mA
Photomonitor current at rated output power		95.0 μA
Spectral width (Full wave, half maximum width at 0.5 mW CW output power at 25 C)		1.10 nm
Thermistor resistance	at 5 C	27.3 kΩ
	at 10 C	20.0 kΩ
	at 15 C	15.5 kΩ
	at 25 C	10.0 kΩ
	at 32 C	7.5 kΩ
	at 40 C	5.0 kΩ
	at 50 C	3.5 kΩ
	at 60 C	2.5 kΩ
Thermoelectric cooler inputs (at 25 C)		
	current	0.64 A
	voltage	0.95 V

H. SUMMARY

Semiconductor laser diodes have evolved into rugged, reliable systems and are now the popular choice for many optical applications. New alloys, innovative structures and efficient construction techniques have produced devices which possess many advantages over other emitters:

- high (10 mW) output power,
- narrow (1 nm or less) spectral linewidth which results in less material dispersion in fibers,
- high coherence which allows for focusing of the output beam to produce high irradiance and
- small active regions to facilitate coupling to single-mode fibers. [Ref. 2:p. 262]

Having introduced the concept of laser light, subsequent chapters in this thesis address the design, implementation and testing of the circuits necessary for the stable, controlled operation of a laser diode.

III. TEMPERATURE STABILIZATION NETWORK

A. THERMOELECTRIC COOLING

1. Peltier Effect

The small dimensions of the laser diode module makes typical methods of cooling impractical or ineffective. Fortunately, the use of thermoelectric cooler (TEC) modules can readily satisfy the need for temperature stability within the small confines of a laser diode package.

TEC modules utilize the Peltier effect, named after the discoverer of this phenomenon in 1834. Peltier found that by passing an electric current through a junction of dissimilar materials, heat could be created or absorbed at the junction, depending on the direction of the current flow. The operation is similar to the carrier movement in the active region of a laser diode (see Figs. 2.1 and 2.5). However, in the case of a TEC, the heavily-doped n- and p-type materials are separated by an electrical conductor.

To create and sustain the cooling effect, the module is reversed biased, as shown in Fig. 3.1. Electrons are pumped from the p-type to n-type region where they are moved from the valence band to the conduction band. Via the classical laws of thermodynamics, work has been done on the electron and therefore energy (i.e., heat) is absorbed and the junction is cooled. As the junction temperature decreases, heat is drawn from the heat source through an electrical insulator (which is also a good thermal conductor). The same process

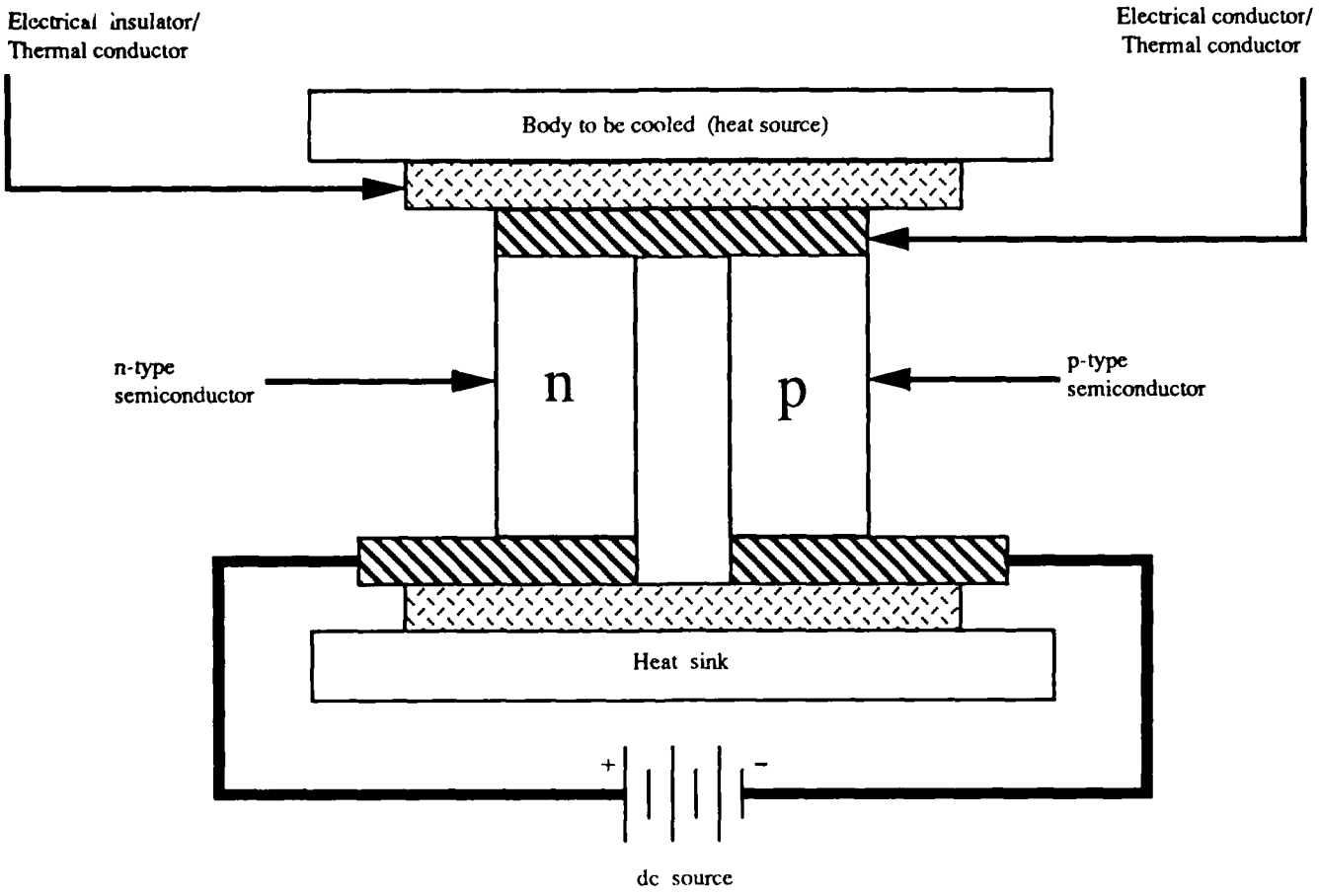

Figure 3.1. Thermoelectric Cooling Couple (from Ref. 18).

holds true for the flow of holes in the opposite direction. Therefore, both carriers work together to remove heat from the junction at a rate proportional to the current applied. In an equal but opposite manner, heat can be produced at the junction by forward biasing the module. By connecting the doped regions in series electrically and in parallel thermally with a sensor and reversible current circuit, the module can heat or cool a system and maintain a stable environment.

Several couples similar to Fig. 3.1 can be joined in parallel or in series (i.e., cascaded) to increase the maximum heat transfer rate and absolute cooling/heating temperature. Single 0.40 cm x 0.40 cm x 0.25 cm couples of doped bismuth telluride, the most common material used, can reduce junction temperatures to well below freezing [Ref. 18]. Cascaded modules can easily arrive at and maintain 65 C temperature differentials and can do so quickly. Current levels of performance can change laser diode temperatures from 25 C to 0 C ($\pm$0.2 C) in 60 seconds while temperature stabilities of $\pm$0.001 C have been achieved [Ref. 19:p. 114].

2. Design Parameters

There are several system parameters that need to be specified prior to selecting a particular TEC device. The available cold surface temperature (T_C, the heat sink temperature) must be established. Since the physical dimensions of the TEC module places the heat sink so close to the heat source, the desired operating temperature is considered equal to T_C; normally this is room temperature or approximately 25 C. The heat source temperature T_H must take

into account the ambient temperature of the environment and the efficiency of the heat exchange action between the hot side of the TEC and the heat sink. The amount of heat removed (absorbed) by the heat sink Q_C must include all thermal loads on the hot side of the TEC. These include the active heat load itself (e.g., a laser diode can produce over 700 mW of heat at 25 C [Ref. 19:p. 110]), conduction and convection losses to or from any surrounding media and radiation from nearby heat sources. In fact, air currents near the heat source are often the limiting factor in maintaining a stable temperature [Ref. 19:p. 114].

The rate at which the load must be cooled will the determine the size of the TEC module needed and the power required. For example, lowering the temperature of a laser diode from 25 C to 0 C would take a 2.0 cm x 3.5 cm x 3.5 cm TEC over 40 s and would require 50 W of power [Refs. 18 and 19:p. 110]. A faster cooling rate would necessitate a larger module and consequently more power.

It also should be noted that TEC devices do not remove or add heat at a constant rate and slow down the exchange process as the heat source approaches the maximum rated temperature differential of the module [Ref. 18]. This maximum differential is material-dependent and is specified by

$$\Delta T_{MAX} = 0.5Z(T_C)^2 \tag{3.1}$$

where T_C is the available cold junction temperature (as stated above) in degrees Kelvin and Z is the specific material's thermoelectric figure of merit. This figure of merit is, in turn, defined for various substances by

$$Z = \frac{\alpha^2}{\rho\kappa} \tag{3.2}$$

where α is the Seebek or thermoelectric coefficient in $V\text{-}K^{-1}$, ρ is the resistivity in Ω-cm and κ is the thermal conductivity in $W\text{-}K^{-1}\text{-}cm^{-1}$. Using the value of Z specified for bismuth telluride ($Z = 3 \times 10^{-3}\ K^{-1}$), ΔT_{MAX} can reach 75 C. The TEC mounted inside the QLM-1300-SM-BH can maintain the laser diode active region at −20 C with an ambient temperature of 65 C. [Ref. 17]

In addition, a desired coefficient of performance (COP) may affect the previous factors. Defined by

$$COP = \frac{Q_C}{Q_{IN}} \tag{3.3}$$

where Q_C is the total amount of heat transferred and Q_{IN} is the total electrical power supplied, the COP establishes the efficiency of heat removal by the exchanger. The higher the COP, the less power is needed for operation and the less total heat (the sum of Q_C and Q_{IN}) needs to be rejected. Higher COP values however, usually mean a higher price per thermocouple. [Ref. 18]

Finally, care must be taken with the dc power source driving the TEC. Any ac ripple in the supply current degrades the cooling effect. The reduction in capability can be approximated by the following

$$\Delta T_{RIPPLE} = \frac{\Delta T_{MAX}}{1 + N^2} \tag{3.4}$$

where ΔT_{MAX} is defined by Eq. 3.1 and ΔT_{RIPPLE} is the maximum differential possible with N percent ripple in the supply current. Armed with this information and the capabilities of the available power supplies, standard performance graphs can be used to determine the size and number of TEC modules needed. [Ref. 18]

3. Reliability

Due to their solid state construction, TEC modules are extremely robust and reliable, despite their small size. As long as the unit is operated within its specified supply current parameters, mean-time-to-failure can exceed 100,000 hours at elevated operating temperatures of 100 C; at room temperature (25 C), this lifetime is doubled or tripled. [Ref. 18]

Due to its physical layout, each TEC is quite resistant to shock, vibration and compressive loading. However, care should be taken when subjecting a module to shear forces. [Ref. 18]

4. TEC Limitations

There are, of course, limitations to the capabilities of any TEC unit which must be taken into account prior to use. The heat sink, i.e., the cold side of the module, must be maintained at or below the desired operating temperature in order to provide a cool surface for proper exchange action. The TEC module should be mounted as efficiently as possible onto the heat source in order to increase responsivity and provide high thermal conductivity. [Ref. 18]

B. CIRCUIT IMPLEMENTATION

1. System Design

Once it has been decided that a TEC will be used, some sort of electronic circuit must be built to regulate the current into the module and maintain a stable heat source temperature. Figure 3.2 is the basic schematic for such a feedback loop. The actual temperature of the source is measured using

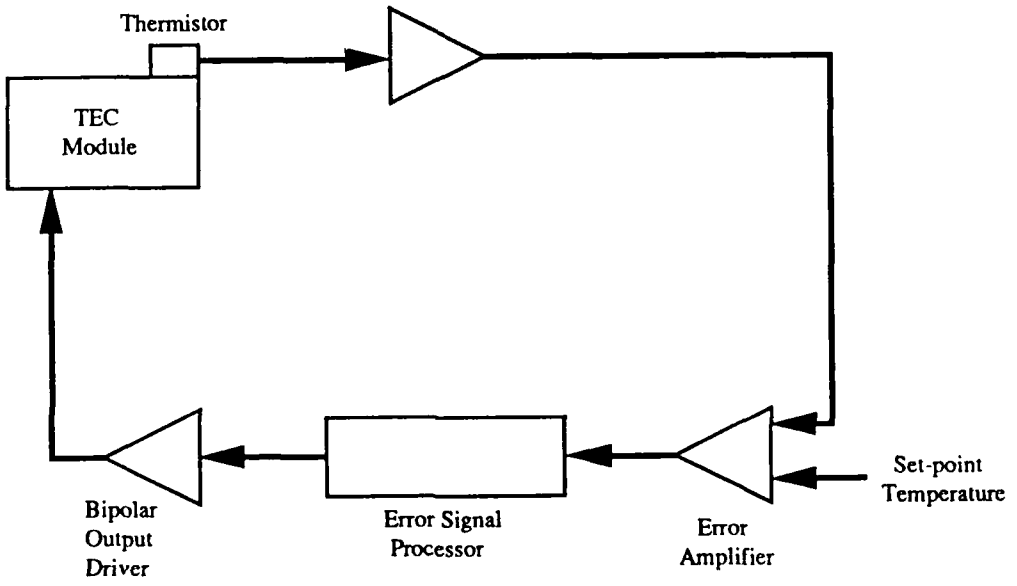

Figure 3.2. Feedback Loop for Temperature Control (from Ref. 19).

a negative-temperature-coefficient thermistor mounted as close as possible to the active heat source. Although these devices are inexpensive, accurate and highly sensitive, their resistance is a nonlinear function of temperature. Figure 3.3 is a graph of the characteristics of the thermistor built into the Lasertron module. The points indicated by the small squares are the data from Table 1; they are simply connected by a smooth curve (the solid line). Using linear regression and

a least-squares fit model, the data of Table 1 was modeled as

$$\text{Temperature} = 70.11 \exp[(-0.0978)(\text{Resistance})] \tag{3.5}$$

and is plotted in Figure 3.3 by the dotted line (with points indicated by circles).

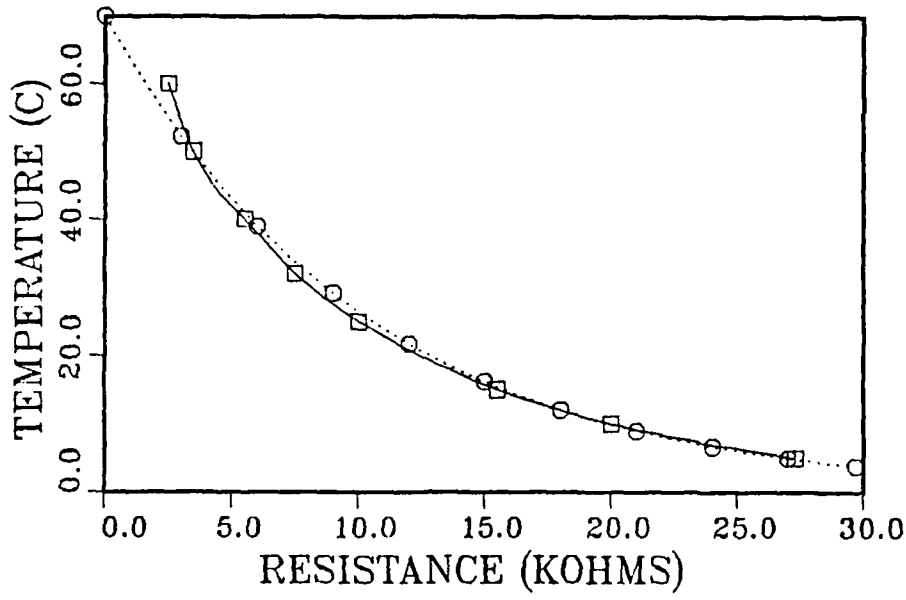

Figure 3.3. Thermistor Temperature versus Resistance.

The close fit indicates the thermistor temperature-resistance relationship is indeed exponential. However, this may not be a problem if temperature swings are not very large; the relationship of resistance versus temperature may be approximated by a straight line for small changes in temperature.

Within the cooling network of Fig. 3.2, the measured temperature (i.e., thermistor resistance) is compared to a set-point temperature (resistance), producing an error signal. The circuitry of Fig. 3.2 implements a form of

$$I_C = A + BE + \frac{1}{C}\int E\,dt + D\frac{dE}{dt} \qquad (3.6)$$

where I_C is the current sent to the TEC, E is the error signal and A through D are constants which depend on the thermal load and the cooling performance required [Ref. 19:p. 113].

Most simple controllers are concerned only with the first two terms of Eq. 3.6. Easily constructed using a bias current and op-amp gain mechanism, the basic controller is designed to produce a fast response with a minimal overshoot to a desired set point (i.e., temperature). However, there always exists a residual error, even after the controller settles to a final state. Although this error could be partially reduced by applying a constant bias current, this technique is practical only when the set-point and device temperatures are relatively constant [Ref. 19:pp. 113-114]. This thesis design is, by choice, to be used with a wide variety of laser diode devices and therefore this basic circuit would not meet the flexibility and stability requirements.

The residual error problem can be solved by adding the third term of Eq. 3.6, the integrator, to the control loop. Once the constant C is determined experimentally (to produce a fast response with minimal overshoot), the network can accommodate a relatively wide variety of thermal loads. Unfortunately, integration of large residual errors can be slow, necessitating the implementation of a complete proportional-integral-differential loop (all four terms of Eq. 3.6). However, as explained in Ref. 19, the occurrence of such large differentials in tightly coupled loads (such as laser diode modules with built-in TECs) is rare, and

the added complexity of the complete circuit is not usually justified. Therefore, the proportional-integral network of Figs. 3.4 through 3.6 was designed for temperature stabilization.

Figure 3.4 shows the supply voltage regulators necessary for the TEC circuit, as well as the other portions of the total design. The decision to use

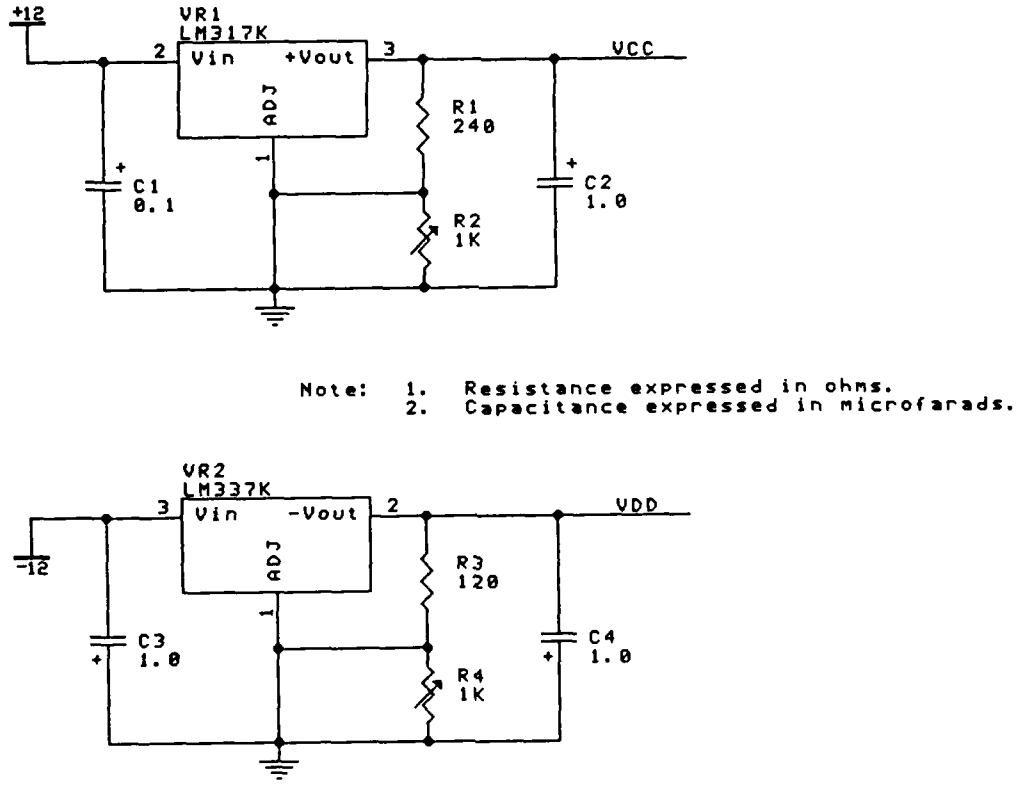

Figure 3.4. Voltage Regulators (from Ref. 20).

large, monolithic devices in later circuits required an external power source of ±15 V dc. Powering the op-amps required ±5 V dc, therefore the LM317 and LM337 voltage regulators were used in accordance with Ref. 20. The cooling circuit also needed a very precise voltage for use by the comparator op-amps,

therefore the source of Fig. 3.5 was constructed to provide a very stable, buffered +2 V dc.

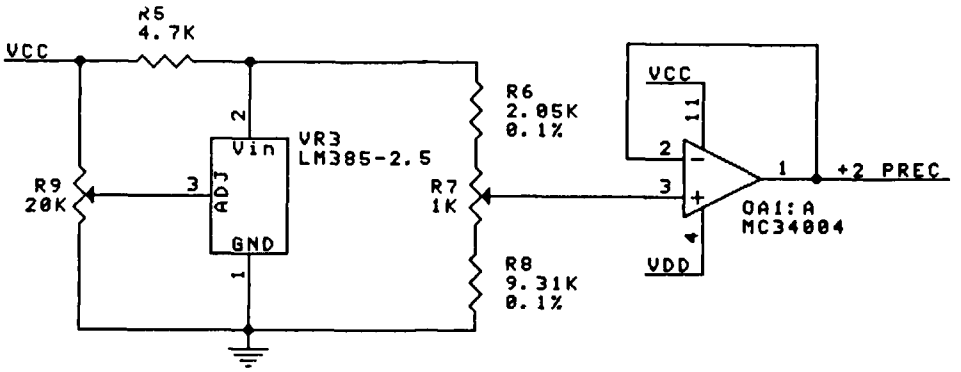

Figure 3.5. Precision +2 V DC Regulator (from Ref. 21).

These regulated voltages were then fed to the circuit of Fig. 3.6 which drives the variable current source for the TEC. The desired operating (set-point) temperature is established by adjusting the potentiometer at R10, and the resulting reference voltage is sent to the inverting input of the comparator network of OA3. The actual laser diode temperature is sensed by the thermistor in the feedback loop of OA2; this "temperature" value is then passed to the comparator. The two values are compared in OA3, producing an output voltage comparable to the difference in temperatures. [Ref. 21]

The feedback loop on OA3 (R24 and C1) helps speed up its reaction to slow variances in the set-point and actual temperature signals, reduces oscillations in the comparator output and eliminates any "dead zones," i.e., small variances between the outputs of OA1 and OA2 which could produce no reaction

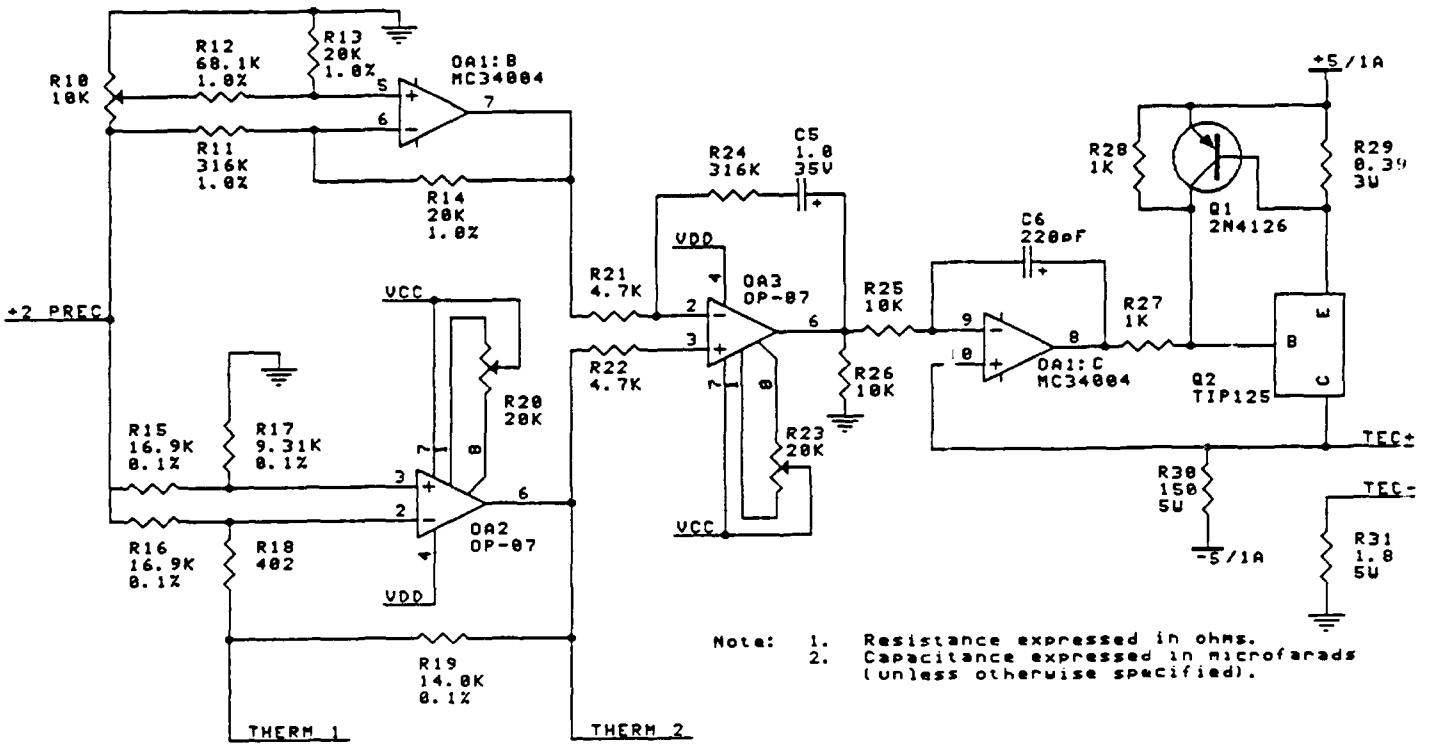

Figure 3.6. TEC Drive Circuit (after Refs. 12, 21 and 22).

(i.e., output) from the comparator [Ref. 22:p. 402]. The error signal from OA3 is integrated by OA1:C and the proper amount of cooling current is fed to the TEC via Q2.

The current is regulated in the following manner. As the thermistor resistance drops, the output of OA2 will increase relative to the output of OA1:B. This in turn will *increase* the output of the difference amplifier OA3. The output of the inverting integrator OA1:C will consequently *decrease*. When this output is negative, Q1 will turn on and positive current will pass to the TEC to cool the laser diode module. By the same analysis, if the thermistor resistance increases *above* the desired set-point level, Q1 is turned off and negative current is fed to the TEC which heats the module. When the inputs to OA3 are equal, the set-point temperature equals the laser diode temperature and no cooling/heating current is passed to the TEC.

A separate ±5 V dc high current source is necessary for the Darlington configuration to operate effectively. Table 1 indicates that the QLM-1300-SM-BH can sustain 0.636 A of cooling current; this is supplied by the ±5 V/1 A sources. The resistance and high wattage values of R29, R30 and R31 ensure the laser module maximum current rating is not exceeded and prevent overload damage to the TEC. With the values of resistance used in Fig. 3.6 and a TEC load resistance of 1.48 Ω (as computed from Table 1), this cooling circuit supplies a range of currents between −0.03 A and 0.62 A.

2. Wiper Voltage versus Temperature Relationship

In order to easily use the circuit of Fig. 3.6, a relationship between the desired set-point temperature and the wiper voltage at R10 must be found. To do this, a dummy 1.48 Ω load was applied across the TEC+ and TEC− terminals in Fig. 3.6. Then several values of resistance were placed across the THERM_1 and THERM_2 terminals; R10 was varied until a voltage swing was noted across the dummy load at the TEC terminals. By measuring the wiper voltage at R10 at the moment the current supply shifted, a relationship between the *desired* temperature and *actual* temperature can be approximated. Table 2 shows the resulting data; it was noted that the current swing for the varying resistances occurred at different points depending on whether the wiper voltage across R10 was changed from high (+2 V dc) to low (0 V dc) or from low to high. This means there is a built-in error in the circuit of Fig. 3.6 which must be taken into consideration during use. The average value of each set of voltages is also shown; this is the value which was used in all subsequent calculations.

TABLE 2. WIPER VOLTAGE VERSUS THERMISTOR RESISTANCE

Thermistor Resistance (kΩ)	Wiper Voltage (V)			
	High-to-Low	Low-to-High	Average	Error
9.96	1.60	1.74	1.67	±0.07
14.76	1.20	1.30	1.25	±0.05
20.49	0.86	0.98	0.92	±0.06
24.68	0.67	0.79	0.73	±0.06
29.80	0.49	0.59	0.54	±0.05
34.20	0.37	0.47	0.42	±0.05

The resistance versus average voltage values of Table 2 were plotted in Fig. 3.7: the data is represented by the squares and is simply connected by a smooth curve (the solid line).

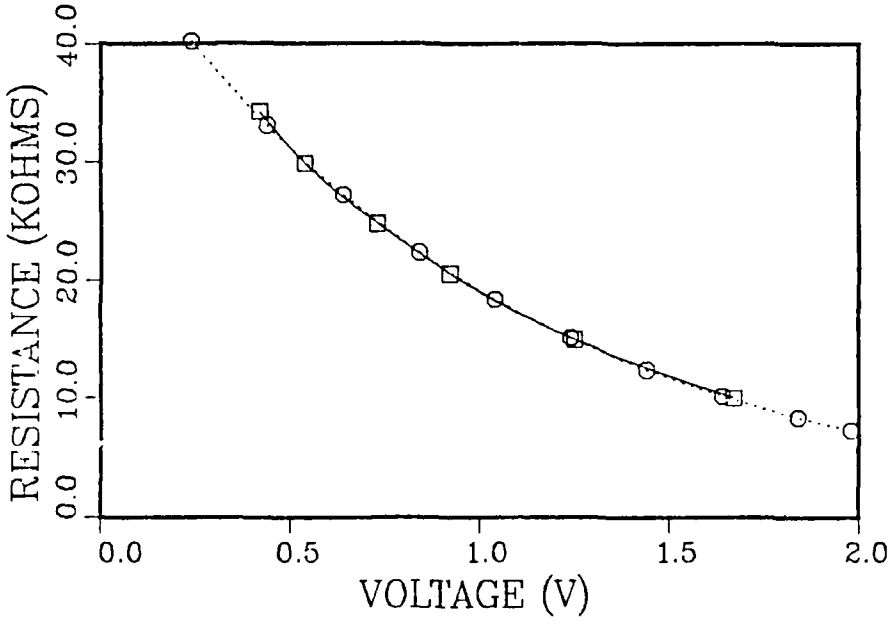

Figure 3.7. Thermistor Resistance versus R10 Wiper Voltage.

Again using linear regression and a least-squares fit, the resistance-wiper voltage relationship was modeled as

$$\text{Resistance} = 50.91 \exp[(-0.983)(\text{Voltage})] \tag{3.7}$$

which is shown in Fig. 3.7 as a dotted line (with points noted as circles). This plot shows that the resistance-wiper voltage relationship is also exponential. By combining Eqs. 3.5 and 3.7, the following relationship is produced

$$\text{Temperature} = 70.11 \exp[-4.98 \exp[(-0.983)(\text{Voltage})]] \tag{3.8}$$

The solid line in Fig. 3.8 (with points noted by squares and connected by a smooth curve) is a graph of Eq. 3.8. By using linear regression and a least-squares fit, a *linear* model of Eq. 3.8 (over the entire range of wiper voltages) was found to be

$$\text{Temperature} = 18.2\,(\text{Voltage}) - 4.78 \tag{3.9}$$

which is plotted as the dotted line in Fig. 3.8 (with points noted by circles). As can be seen, there is not a very close match between this first model and the predicted relationship of Eq. 3.8. However, it can be seen that the predicted relationship of Eq. 3.8 is nearly linear for R10 wiper voltages greater than 1.25 V dc. Therefore, by using linear regression and a least-squares fit on the *near-linear* portion of Eq. 3.8, the second modeled relationship was found to be

$$\text{Temperature} = 25.0\,(\text{Voltage}) - 15.0 \tag{3.10}$$

which is shown by the dashed line in Fig. 3.8 (with points indicated by triangles). There is obviously a much better match between the second model and the linear portion of the predicted relationship of Eq. 3.8; there is, of course, an ever-increasing error as the desired set-point temperature is lowered below approximately 15 C (*i.e.*, reducing the R10 wiper voltage below 1.25 V dc). Since the Lasertron laser diode module will probably be operated at or near room temperature (25 C), which is well within the linear portion of the predicted relationship, Eq. 3.10 could be used as an accurate representation of the set-point temperature versus R10 wiper voltage relationship.

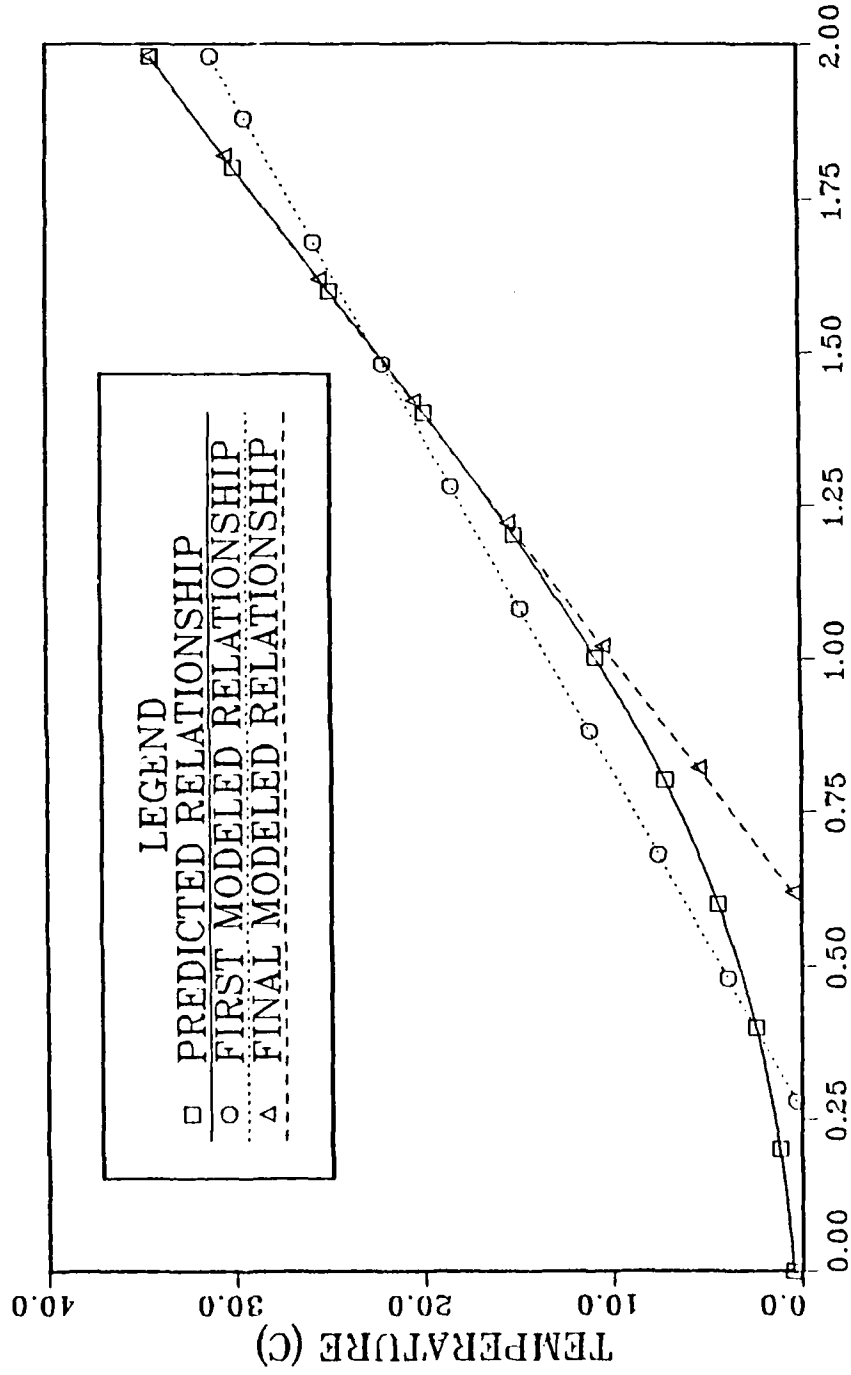

Figure 3.8. Set-point Temperature versus R10 Wiper Voltage.

3. System Flexibility

The network of Figs. 3.4 through 3.6 may be used for other TECs with higher/lower current ratings by:

- increasing/decreasing the output of the high current source or
- decreasing/increasing the series resistance R31.

However, care must be taken to ensure that:

- the maximum current and voltage levels of the TIP125 Darlington and 2N4126 PNP transistor are not exceeded,
- the TIP125 Darlington is adequately heat-sinked and
- the high current source is not overdriven.

C. SUMMARY

The capabilities of thermoelectric coolers have allowed designers to maintain the compact size of operational laser diode modules while, at the same time, maintaining the necessary temperature control. By creating a controllable environment for electroluminescence, not only can the optical output be maintained at stabilized levels in spite of operating temperatures, but

- the output wavelength can be precisely "tuned" through a small range of values and
- compensation for gradual degradation (i.e., aging) can be effected by increasing the amount of cooling, thereby extending the useful lifetime of the laser diode.

IV. POWER STABILIZATION NETWORK

A. REQUIREMENTS FOR STABILIZATION

Chapter II described the effects of gradual degradation on the performance characteristics of a laser diode. Two major reasons for these losses are age and heat. Figure 4.1 demonstrates the effect of these changes in the power-current curve of a typical device. As the laser diode ages (or temperature increases) from time t_1 to t_2 to t_3, the output curve shifts to higher threshold currents as well as

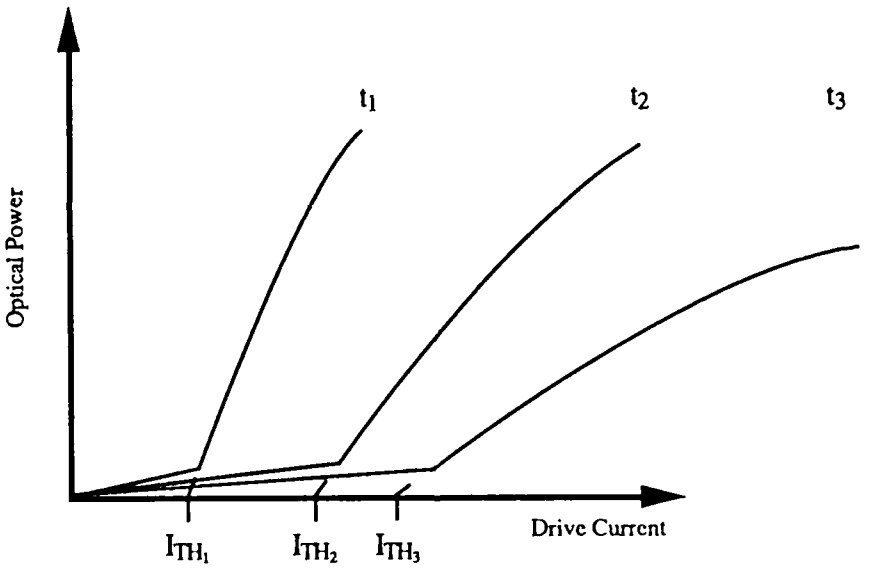

Figure 4.1. Effect of Aging and Heat on Optical Output (after Ref. 2).

decreases slope. To combat the effects due to heat, the network in Chapter III was designed to maintain a stable operating temperature. The cooling circuits could also compensate for slight aging effects; i.e., the set-point temperature could

be lowered *below* the desired operating point until the required optical power levels were achieved.

However, cooling cannot completely stabilize the laser diode's output nor can it correct for severe aging problems. In addition, Ref. 17 states that the thermoelectric cooler response time within the laser module used for this design is typically 30 s; such a delay could be fatal to the device. Therefore, a separate network is needed which can measure the *actual* optical power from the laser diode, compare the values to *desired* levels and to modify the drive current to produce the correct output.

Figure 4.2 is a block diagram of such a network. A photodiode monitors the output of the laser diode and produces a current linearly proportional to the radiated optical power. This current is changed to a voltage via a transimpedance amplifier. This voltage is then simultaneously analyzed to verify the average optical power and maximum amplitude variation of the output analog signal.

The dc bias voltage of the output signal is compared with a voltage representing the desired average power. The difference will drive an integrator which will increase or decrease its output as necessary until the measured dc bias matches the desired level.

The output of the transimpedance amplifier, after passing through a coupling capacitor to remove the dc component, is analyzed to determine the *maximum* peak-to-peak fluctuation of the optical signal. The ratio of the actual variationto required variation is multiplied by the actual analog signal to create a voltage which will produce the desired power modulation.

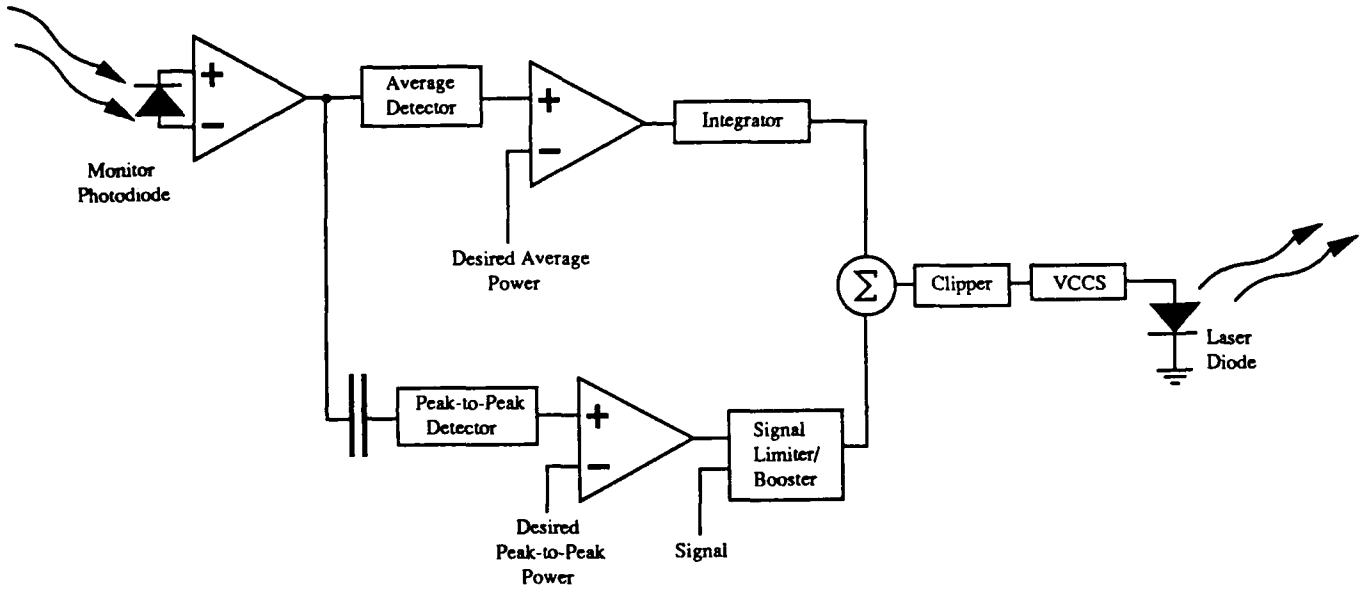

Figure 4.2. Power Stabilization Network (after Ref. 2).

The bias and modulation voltages are first summed and then checked by a series clipper to prevent an overload signal being sent to the laser diode and to avert the possibility of a catastrophic degradation. This clipped voltage is then converted to a current to drive the laser diode at the desired power levels.

B. PHOTODIODE CURRENT-TO-VOLTAGE CONVERTER

1. Photodiode Operation

The function of any photodiode (PD) is to convert incident optical power into an electrical signal. As discussed in Refs. 2:pp. 326-347 and 7:pp. 147-162 a current is produced by the reverse-biased device (i.e., in a photoconductive mode), a technique which is the reverse of the electroluminescence phenomenon discussed in Chapter II. Regardless of the type of construction (pn, pin, avalanche, etc.), the output of a PD typically corresponds to the curve of Fig. 4.3. Although the data used to construct Fig. 4.3 is derived from Table 1, the transfer characteristic of most PDs can be represented by such a straight line, a relationship which does not vary appreciably with age or temperature [Ref. 23:p. 176]. The power stabilization network developed in this chapter depends only on the responsivity **R** of the PD at the emitted wavelength of the LD being monitored. This performance characteristic (or energy conversion efficiency) is defined as

$$\mathbf{R} \equiv \frac{I_{out}}{P_{inc}} \tag{4.1}$$

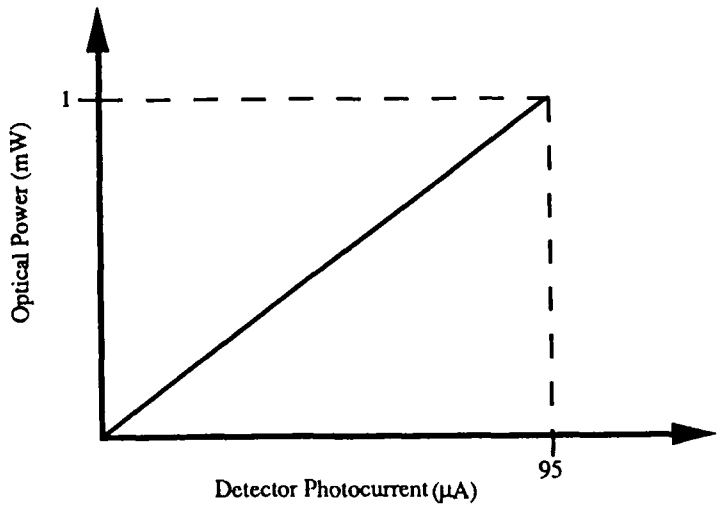

Figure 4.3. Photodiode Current versus Optical Power (after Ref. 17).

where P_{inc} is the optical power incident on the PD, and I_{out} is the PD output current at that level of incident power. As shown in Eq. 4.1, using the data from Table 1, the integral PD in the Lasertron module has a responsivity of approximately 0.1 A-W^{-1}. In this instance, the dark current (i_d) of this particular PD is ignored, since it is nominally less than 0.1 μA [Ref 17]; however, care must be taken as the module temperature changes, which can double i_d for every 10 C increase [Ref 7:p. 154]. Extremely small optical signals (in this case those less than 10 μW) could be lost in the dark-current noise.

2. Transimpedance Amplifier

The second half of the receiver circuit is the preamplifier which is used to linearly change the PD current into a voltage. This voltage is then analyzed by subsequent stages to produce a stabilized drive current. Figure 4.4 is the transimpedance circuit which begins the stabilization network. Compared with

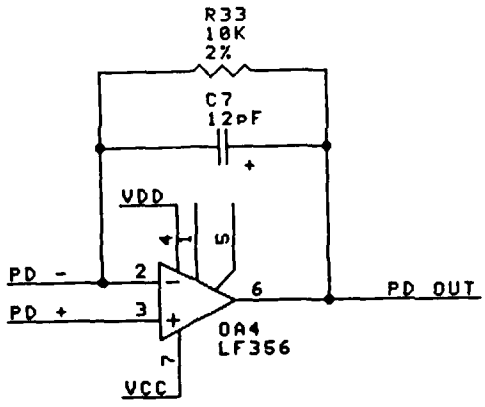

Note: 1. Resistance expressed in ohms.
2. Capacitance expressed in microfarads (unless otherwise specified).

Figure 4.4. Transimpedance Amplifier (after Ref. 22).

other current-to-voltage converter options (bipolar, FET, or high-impedance receivers), the transimpedance amplifier has a wide dynamic range and requires a relatively simple electronic circuit (with no frequency equalizers necessary) [Ref. 7:p. 258]. These characteristics make it ideal for such applications.

The output signal V_{out} of this receiver is described as

$$V_{out} = (I_{PD})(R33) \tag{4.2}$$

where I_{PD} is the monitor photodiode output current and R33 is the feedback resistor across the transimpedance amplifier of Fig. 4.4. PD_OUT is the voltage which represents the power output of the laser diode being monitored. Using the data from Table 1, it was noted that the PD in the Lasertron module produces a current ranging approximately between 0 and 100 μA to represent an output power difference of 0 to 1 mW; therefore, for convenience, R33 was chosen to produce a PD_OUT range of 0 to 1 V for this current swing.

One problem with this circuit is the potential for thermal noise from the feedback resistor R33. However, the noise from the transimpedance configuration is less than most other receivers (except the high impedance option) and the relatively low value of R33 reduces this problem even further [Ref. 7:p. 258].

C. DRIVE CURRENT COMPENSATION CIRCUITRY

1. Output Bias Sensor

Once the photodiode current is converted to PD_OUT, the voltage is analyzed to determine the actual dc component (i.e., bias level) of the laser diode's optical output. The upper half of Fig. 4.5 is the circuit used to produce a dc voltage comparable to the drive current bias. The voltage-follower configuration of OA5 provides buffering between the transimpedance amplifier of Fig. 4.4 and the rest of the compensation circuit. The low-pass filter network of R36 and C7 then extracts the voltage ACT_BIAS which represents the dc component of PD_OUT. The value of C7 was chosen large enough to maintain a near constant bias value without oscillations over a relatively long period of time; the charging period for such a capacitor is not a factor in this circuit since turn-on delay safety requirements for the laser diode will exceed this time span.

The second voltage follower OA6 provides additional buffering, and the offset nulling action of R37 compensates for any losses in this network.

2. Signal Peak-to-Peak Sensor

The voltage from the transimpedance amplifier is also analyzed to measure the maximum fluctuation of the photodiode output (i.e., the maximum

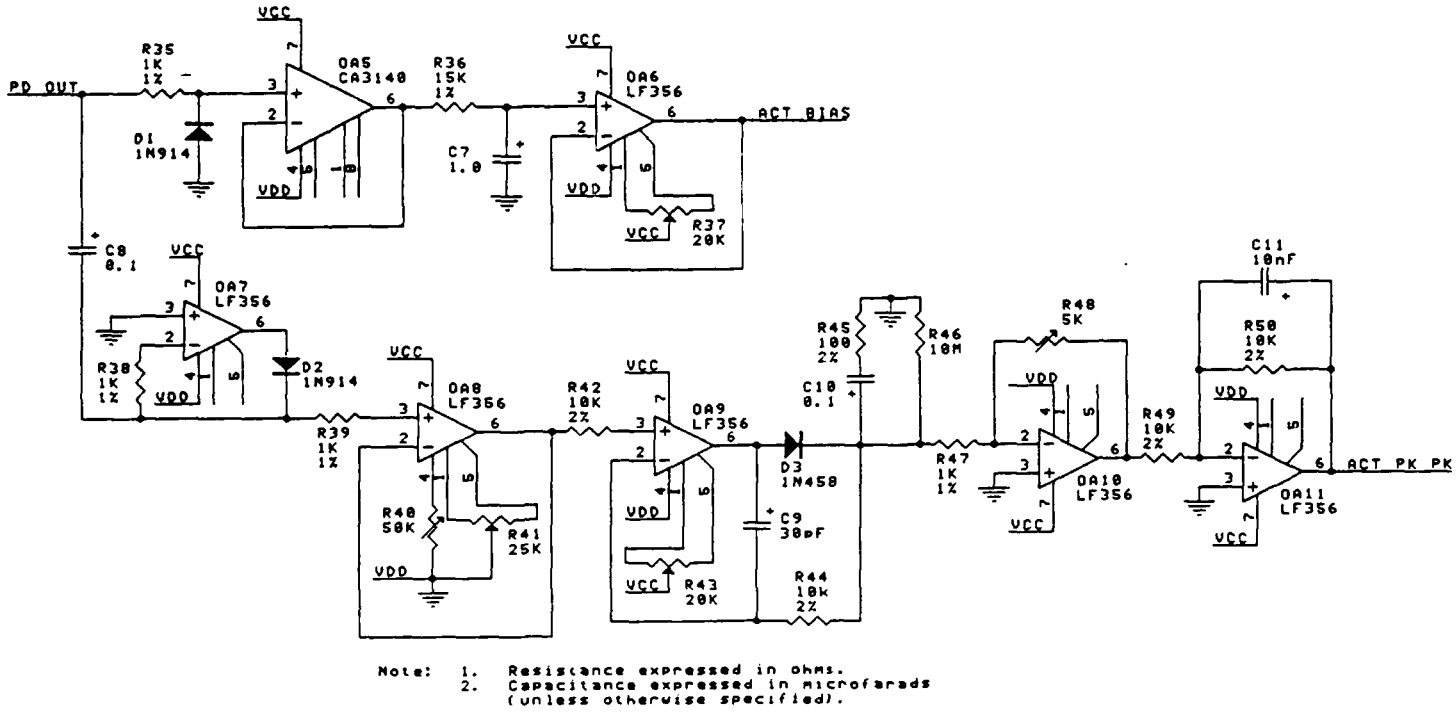

Figure 4.5. Photodiode Output Analyzer (after Ref. 22).

peak-to-peak variation of the optical output signal). Referring again to Fig. 4.5 (and as discussed in Ref. 22:pp. 232-233), the voltage PD_OUT charges the coupling capacitor C8 and thereby clamps this signal's peak negative value to zero (i.e., ground). When PD_OUT swings negative, OA7 drives D2 on, maintaining the charge of C8. When the negative peak has passed and D2 has turned off, the charge of C8 is still maintained since the only current drains are the inputs to OA5 and OA6 (typically 30 pA) [Ref. 24: p. 3.2]. This results in a fast-charge, slow-decay response to changes in the *maximum* fluctuation of PD_OUT.

If the ac component of PD_OUT is relatively large or small, the circuitry with OA7 and OA8 may not be able to accurately clamp the signal to ground, thereby resulting in a *biased* waveform being measured for peak values by follow-on circuitry. Figures 4.6 through 4.8 demonstrate this problem.

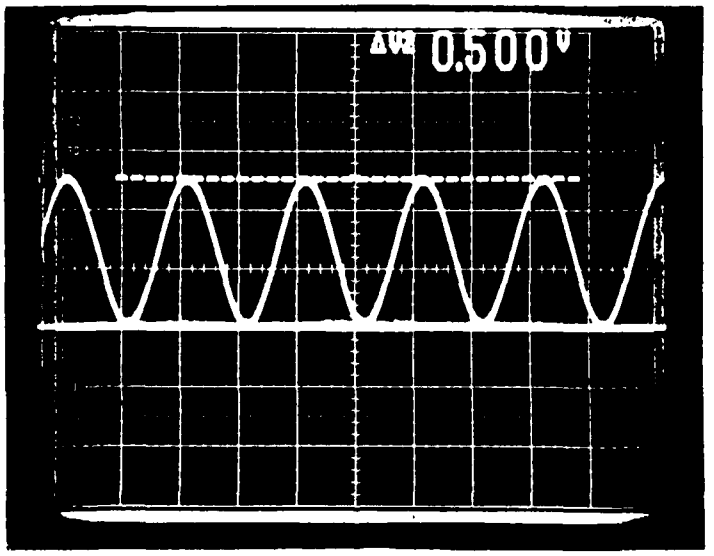

Figure 4.6. Properly Clamped Signal.

Figure 4.6 is a properly clamped waveform; the most negative peak of the sine wave is held at ground (the solid line). The actual signal amplitude is 0.5 V and the circuitry will produce that value.

If the amplitude of the wave is too small, as in Fig. 4.7, the negative

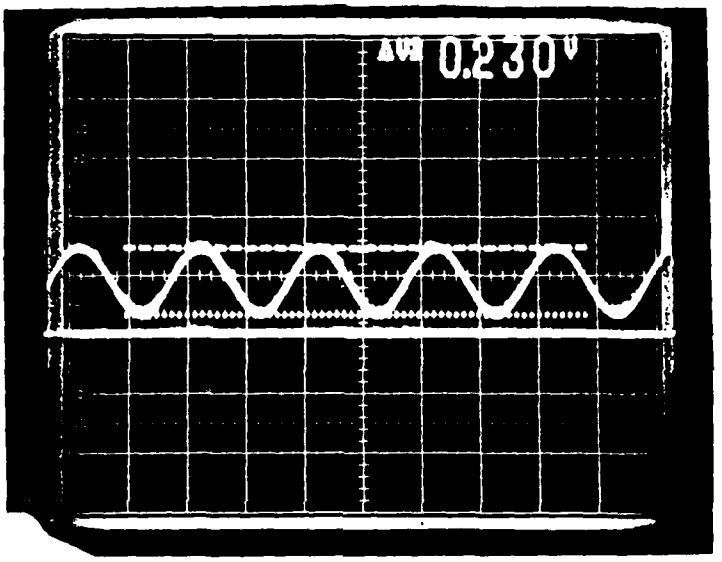

Figure 4.7. Signal Clamped Above Ground.

peak may not be clamped to ground, producing an error in the measured peak-to-peak fluctuation. The measured value is *more* than the actual peak-to-peak, therefore the compensated drive signal would have *less* fluctuation than desired. As shown in Fig. 4.7, the actual signal amplitude is 0.230 V; however the circuit will measure a peak-to-peak difference of 0.295 V which includes the amount of offset (+0.065 V) in the clamped signal.

If the amplitude is too big (as in Fig. 4.8), the circuit could measure a peak-to-peak fluctuation that is *less* than the true value, forcing the compensated

drive current to be *more* than is desired. The 0.775 V peak-to-peak signal in Fig. 4.8 would be measured with a 0.725 V amplitude due to the negative offset (approximately −0.050 V) in the improperly clamped waveform.

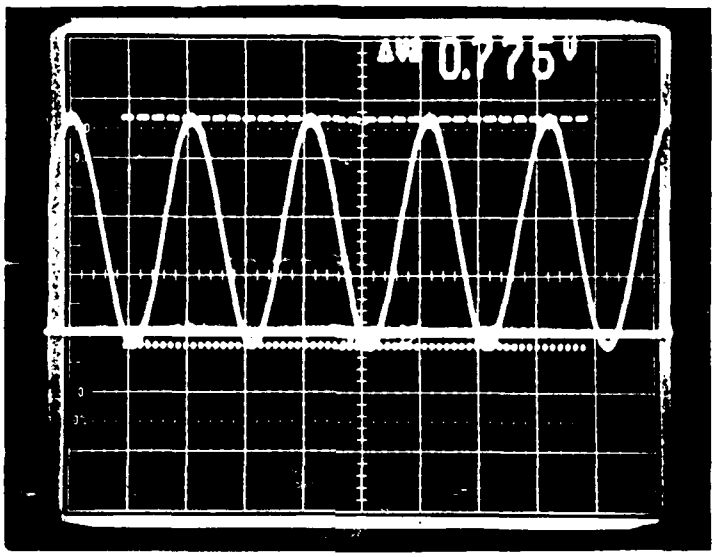

Figure 4.8. Signal Clamped Below Ground.

Therefore, R40 and R41 are provided to allow precise clamping of PD_OUT to ground. Varying the negative supply voltage to OA8 via R40 performs large, coarse adjustments to the clamp, while R41 fine-tunes the balance to precisely adjust the clamping. By monitoring the output of OA8 during operation, proper clamping action can be verified. If this is not possible, R40 and R41 can be preset to produce acceptable performance over an *a priori* (or likely) range of fluctuations.

For example, according to Table 1 the Lasertron output power ranges between 0 and 1.0 mW; this corresponds to a photodiode current of 0 to 95.0 μA which results in a PD_OUT voltage from Fig. 4.4 of approximately 0 to 1.0 V.

After adjusting R40 and R41 to the median expected signal (i.e., 0.5 V from PD_OUT), accurate clamping of peak-to-peak signal amplitudes between 0.370 V and 0.735 V (a −26% to +47% range in *maximum* signal values without noticeable error) can still be realized. This median value can, of course, be changed as required. However, care must be taken to ensure the negative swing of the analog signal does not drive the laser diode drive current below its specification-sheet threshold value. Although this stabilization network will compensate for changes in I_{TH} due to aging and heat, user-specified peak-to-peak levels which are too large or bias settings which are too low will adversely affect the action of this circuitry.

The clamped signal can now easily be measured to determine the maximum PD_OUT voltage differential, which represents the maximum optical output difference from the laser diode. In Fig. 4.5, C10 is used to store a dc voltage equal to the peak of the clamped signal from OA8. To accomplish this, OA9 drives D3 on when the slope of the clamped signal goes positive; the rising signal charges C10 to the peak voltage and the capacitor holds this value even when the slope of the clamped input goes negative. As recommended in Ref. 22:p. 254, C10 is made of polystyrene to ensure low leakage and low dielectric absorption and thereby to accurately maintain the desired peak voltage value.

The bleed resistor R46 is used to develop another fast-charge, slow-decay response. Circuit settling times are minimized by C9; configured as shown in Fig. 4.5, the circuit arrives within 0.1% of the true peak value within 10 μs or

less. Finally, R44 helps to prevent overdrive damage to OA9 from C10 when the supply voltages are switched off. [Ref. 22:pp. 254-255]

Two inverting gain amplifiers, OA10 and OA11, are used to compensate for losses within this peak-to-peak detector circuit (and within follow-on stages) and to maintain (with the help of C11) a stabilized dc output [Ref. 22:p. 402]. Together they produce ACT_PK_PK, the voltage which represents the maximum fluctuation in optical power detected by the photodiode in the laser diode module.

3. Bias Compensation Circuit

Once the actual signal bias level is measured (as represented by the voltage ACT_BIAS from Fig. 4.5), this value must be compared to a *desired* output bias level. This comparison is used to produce a *compensated* bias signal which represents the amount of drive which must be supplied to the laser diode in order to increase or decrease the optical output to achieve the desired bias level. Although this circuit produces a compensated *voltage*, this *voltage* is converted into a drive *current* by a voltage-controlled current source in a subsequent stage. Figure 4.9 is the circuit used to produce this compensated dc signal.

The desired bias level is set by R52; using the components shown, the wiper voltage swing is 0 to 1.0 V, which represents a 0 to 1.0 mW output signal bias variation. To increase/decrease this range, R51 can be decreased/increased. The differential amplifier configuration of OA12 produces a voltage comparable to the difference between the actual and desired optical power bias levels. Care

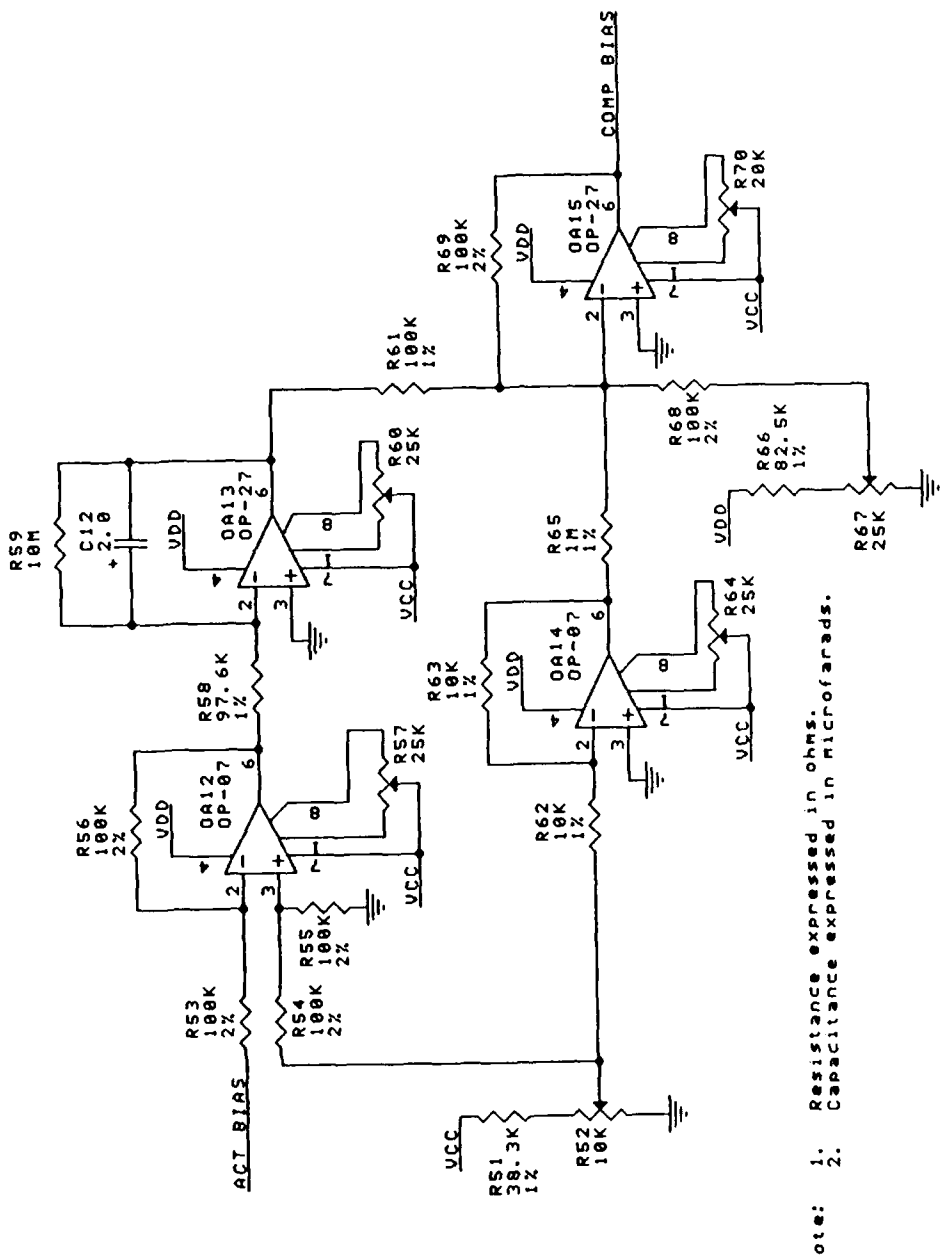

Figure 4.9. Bias Compensation Circuit (after Ref. 22).

must be taken when setting the desired bias; the level must be high enough to ensure that the minimum signal peak does not go below the threshold current (and shut the laser off during operation), and the level must low enough to prevent the drive current from forcing the laser into the thermal runoff region of its power curve (see Fig 2.2).

The output of OA12 feeds the continuous integrator of OA13. As long as the difference between desired and actual bias levels (i.e., the output of OA12) is non-zero, the voltage across C12 will increase or decrease at a rate proportional to this difference. The voltage (E_{out}) at the output of OA13 is therefore

$$E_{out} = -\frac{1}{(R58)(C12)} \int_0^t E_{diff}\, d\tau \tag{4.3}$$

where E_{diff} is the differential voltage at the output of OA12. The "gain" of this integrator, the rate of change of E_{out}, is defined as

$$\text{Gain} \equiv \frac{1}{(R58)(C12)} \cong 5\frac{V}{sec} \text{ per Volt input} \tag{4.4}$$

Although not critical for this stabilization application, this "gain" allows the integrator to quickly follow the gradual degradation (or the *desired* change) of the laser diode's output bias level. The shunt resistor R59 introduces dc feedback to stabilize the integrator's operating point and to reduce the likelihood of saturating OA13. [Ref. 22:p. 430]

The desired bias level set by R52 is first inverted (by OA14) before being applied to the summing-invertor amplifier of OA15. The gain of -10

induced by R65 and R69 (*negative* gain since this voltage will be applied to a summing-*invertor* amplifier) is due to the current-to-optical power ratio of the diode during lasing. Table 1 indicates that this ratio for this particular device is approximately

$$\frac{\Delta I}{\Delta P} = \frac{45\ \text{mA} - 35\ \text{mA}}{1\ \text{mW}} = 10\ \text{A-W}^{-1} \tag{4.5}$$

Consequently a gain factor of 10 is used when formulating the desired bias level (which is actually represented in mW) and computing the required drive current. If this current-to-power ratio is different than 10:1 for the laser diode being used with this circuit, R65 must be altered as needed to produce the expected results.

A voltage which corresponds to the laser diode's threshold current is set by R67 in Fig. 4.9. The wiper voltage can vary between −1.0 V and 0 V which represents a threshold current range of 0 to 100 mA (the variation is over negative voltage since this will be used in a summing-*invertor* amplifier); this range can be increased/decreased by decreasing/increasing R66. This value of threshold current is obtained from the particular laser diode's specification sheet (e.g., Table 1) and is set during circuit start-up procedures.

Finally, these three representative voltages--the desired bias level, the difference between the desired and measured levels and the value representing a particular laser diode's threshold current--are summed in OA15. The result is the voltage COMP_BIAS which corresponds to the *compensated* bias current level necessary to achieve the desired average optical output from the laser diode.

4. Automatic Gain Control Circuit

In order to achieve the desired maximum peak-to-peak fluctuation in the optical output of the laser diode, the peak *measured* variance (from the circuit in Fig. 4.5) must be compared to a *desired* value, and the actual modulation input amplified or attenuated accordingly. These comparisons and modifications are accomplished by the circuit in Fig. 4.10.

The desired maximum swing in optical power is set by R71; the wiper voltage varies between 0 and 0.1 V, representing a power variation between 0 and 1.0 mW. The range of voltages representing this desired value is one-tenth the range of ACT_PK_PK, the true power variance; this increased gain factor of ten is inherent in the output of the divider configuration of OA16 [Ref. 25:p. 6.18]. This range can be increased/decreased by decreasing/increasing R72. Again care must be taken when setting the desired peak-to-peak variation; the fluctuation must not allow the laser to shut off (i.e., force the drive current below threshold) or to enter its thermal runoff region (see Fig. 2.2).

The output of OA16 represents the ratio of the desired peak optical power fluctuation to the measured value. This ratio can be as large as ± 10 and is limited only by the electrical capabilities of the AD534 [Ref. 26:p. 6.28]. However, the inputs of OA17 are restricted to the range of ± 1.0 V [Ref. 25:p. 6.44]. Therefore, the output of OA16 is sent through a voltage divider (R73 and R74) to ensure that OA17 is not overdriven.

The computed ratio is then used to modify the actual input signal (applied across pins 1 and 2 of OA17) via the wideband, dc-coupled multiplier

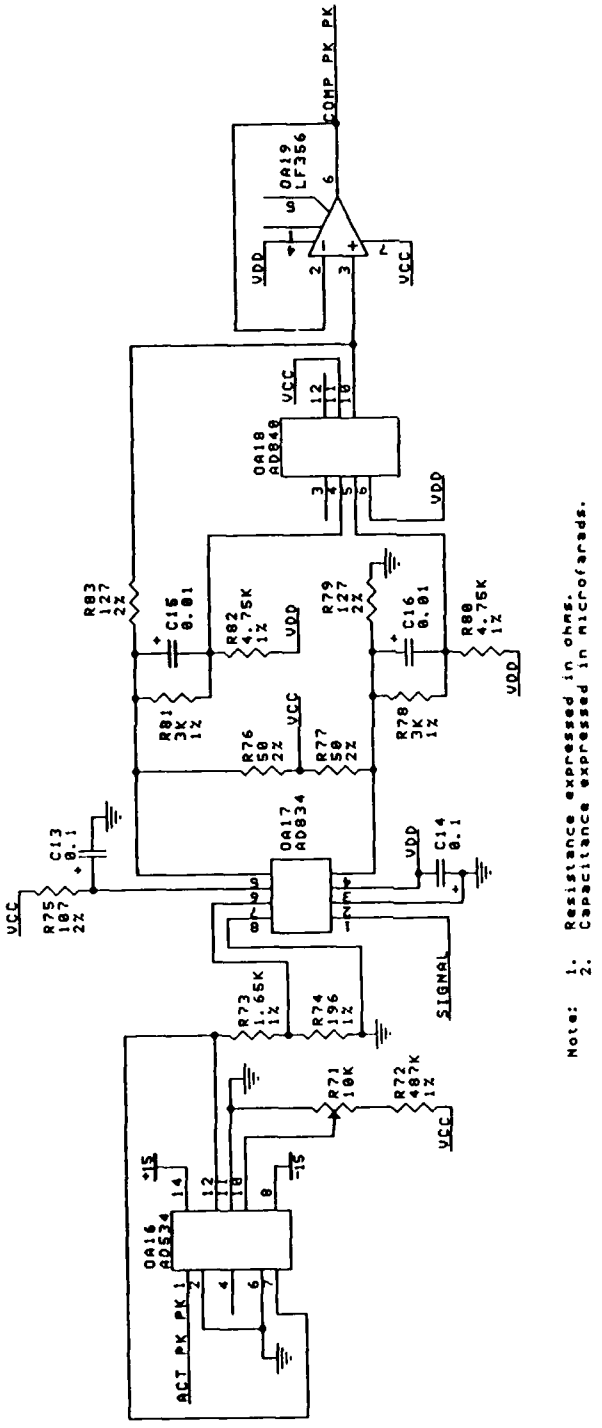

Figure 4.10. Automatic Gain Control Circuit (after Ref. 22).

network of OA17 and OA18. Since inputs of OA17 are limited to ±1.0 V (as noted above), an input signal fluctuation of 1.0 V should correspond to the maximum output power swing from the laser diode being driven. In this design case, using the Lasertron specifications described in Table 1, a 1.0 V peak-to-peak input signal would represent a 1.0 mW optical signal fluctuation. As an illustrative example, if a peak-to-peak fluctuation of 0.5 mW was required from the laser diode, the wiper voltage of R71 would be adjusted to 0.05 V and the input signal would require a peak-to-peak fluctuation of 0.5 V. The compensation circuitry would then modify the input signal to take into account the module's aging and temperature effects as noted by the current from the monitor photodiode. If the peak power of the laser diode is different than the Lasertron being used in this design, the 1.0 V peak input could readily represent a larger (or smaller) maximum optical output by changing certain amplifier resistors in the subsequent final summing amplifier stage.

It must be noted that this network is *not* designed to modify the *input modulation signal*, i.e., to amplify (or attenuate) a weak (or strong) electrical signal. Although the automatic gain control circuitry can be used to artificially boost a weak input signal, the system is intended to stabilize the optical output of the laser diode being driven; it *assumes* that the incoming electrical signal from the signal generator is of the correct strength to produce the desired peak-to-peak power fluctuation; i.e., if a 0.5 mW peak-to-peak fluctuation is desired, an input signal of 0.5 V is assumed at pins 1 and 2 of OA17.

As configured in Fig. 4.10, the full-scale swing at the output of OA18 is ±1.0 V and is accurate to within 1% [Ref. 25:p. 6.47]. Due to the divider network of R73 and R74 and the gain in the OA17 and OA18 circuitry, this voltage represents one-fifth the necessary signal to drive the laser diode and achieve the desired optical power fluctuation. The signal is amplified in the next stage.

The voltage-follower configuration of OA19 provides for stabilization of the compensated input signal and helps to impedance-match the circuit of Fig. 4.10 to the final summing stage.

5. Final Summing Circuit

All that remains to be done in the compensation circuitry is to combine the bias and modulation signals in a summing network. Figure 4.11 is such a network, with the compensated signals COMP_BIAS and COMP_PK_PK being

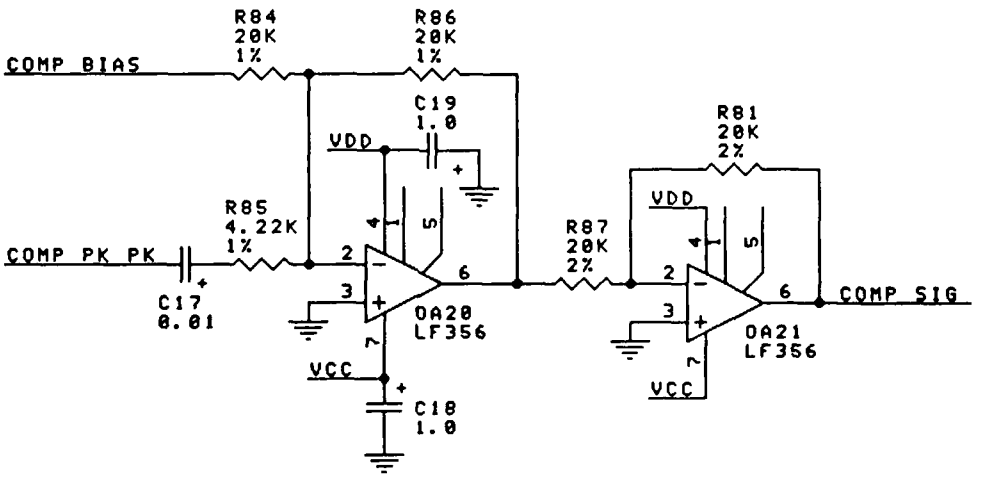

Figure 4.11. Final Summing Circuit (after Ref. 22).

combined in the summing-invertor OA20. Resistors R85 and R86 supply the gain which is required for the amplified peak-to-peak signal as discussed in the paragraph above; the coupling capacitor C17 removes any stray dc signal which may be in COMP_PK_PK. It is R85 which can be changed to produce different power fluctuation levels for 1.0 V inputs to OA17 (see Fig. 4.10); a laser diode with a peak output power of 3.0 mW would use a value one-third of that shown for R85 in Fig. 4.11, a peak power of 0.5 mW would need a resistor twice that shown, and so on. Obviously, the specification sheet of the laser diode being driven must be referenced and the proper value of R85 inserted prior to operation in order to maintain the proper relationships between desired power fluctuation as set by R71, the peak-to-peak fluctuation of the input signal and the optical output of the laser diode.

Finally, since OA20 creates an inverted signal, OA21 is used to produce the necessary positive waveform COMP_SIG.

D. DRIVE "CURRENT" LIMITER

In order to provide overload protection for the laser diode, the series clipping circuit of Fig. 4.12 is included in stabilization network. The wiper voltage of R89 is used to set the "current" limit; since the signals being processed are voltages, this circuit does not really limit current but limits the voltage which will be used to *produce* the drive current in the next stage. The wiper of R89 can vary between 0 and 5.0 V, corresponding to a current limit range of 0 to 500 mA; care must therefore be taken to set a proper limit so as not to negate the effect

of the series clipper. The range of limits can be decreased by including a resistor between R89 and VCC or can be increased by using a higher voltage than VCC sourcing R89.

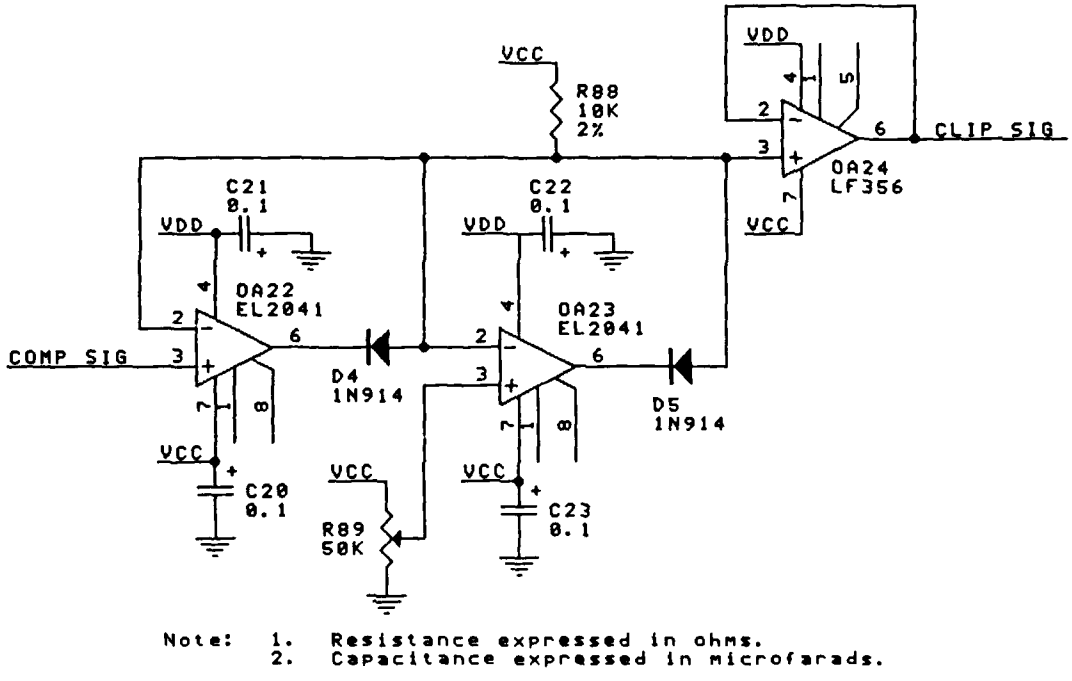

Figure 4.12. Drive "Current" Limiter (after Ref. 22).

The two diodes (D4 and D5) connected to OA22 and OA23 perform a gating function for the compensated signal, allowing whichever voltage (COMP_SIG or the limit set by R89) is *less* to pass to the input of the voltage follower OA24; this combination is therefore labelled the "Linear-OR Gate" [Ref. 22:p. 229]. Whenever COMP_SIG falls below the set limit, OA23 turns D5 off and COMP_SIG is passed directly through to OA24. If COMP_SIG exceeds the limit, OA22 turns D4 off and the set limit voltage appears at the voltage follower OA24.

To realize a high-speed (100 kHz or more) clipper, OA22 and OA23 must necessarily have extremely fast response times and slew rates to produce the proper clipped, compensated drive signal (CLIP_SIG) to the next stage. The EL2041, with a 90 MHz bandwidth, 250 V/μs slew rate and 90 ns settling time (to within 0.05% of final value), is ideal for this application [Ref. 27:p. 1.135].

Figure 4.13 demonstrates the results of this clipping circuit; the wiper voltage

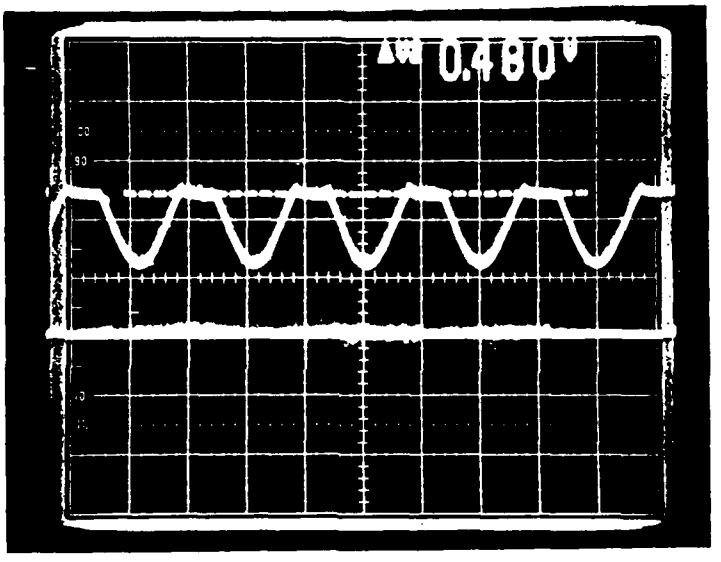

Figure 4.13. Clipped Signal.

of R89 was set at 0.480 V (corresponding to a current limit of 48.0 mA). The minimum overshoot noted in Fig. 4.13 (0.020 V) was constant for all clipping limits. Excellent response was achieved for high speed signals (here at 100 kHz) due to the capabilities of the EL2041 used for both OA22 and OA23.

E. SURGE PROTECTION

Laser diodes are extremely susceptible to current spikes which may appear in the drive current; therefore, some buffering is needed between the network's external power supply and current-producing stage. This buffer acts as a "slow-on slow-off" network to prevent these surges from reaching the laser diode during powering up/down of the circuits or in the case of an unscheduled power interrupt.

Figure 4.14 demonstrates the desired supply voltage-versus-time relationship

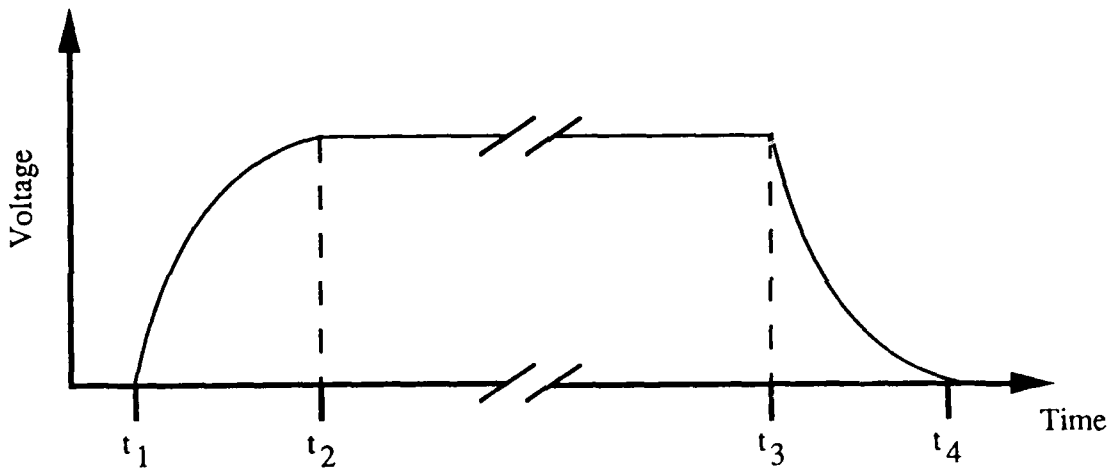

Figure 4.14. "Slow-on Slow-off" Power Supply.

for the surge protector. At some time t_1, external power is connected to the circuit (i.e., turned "on"), and the output of the slow-start circuit "slowly" increases to its maximum value (+15 V for this network) at t_2. The term "slowly" is relative; current spikes are on the order of a few pico- or nanoseconds in duration and voltage transients usually disappear after a few milliseconds, therefore several milliseconds delay between t_1 and t_2 will be sufficient to prevent harmful surges.

At t_3, power is disconnected (either intentionally or not) and the "slow-off" system "gradually" reduces (again during a few milliseconds) the voltage to 0 V.

Figure 4.15 is derived from Ref. 20:p. 2.14. By closing switch S1, LED L1 indicates external power is connected; consequently L1 acts as an indicator of

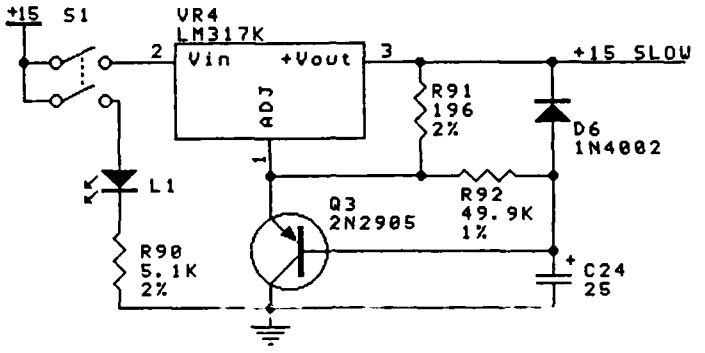

Figure 4.15. "Slow-on Slow-off" Circuit (after Ref. 20)

power failure. Simultaneously, regulator VR4 slowly charges C24. When S1 is opened (or the +15 V power is otherwise interrupted) C24 slowly discharges through the Q3, VR4, R91, R92 and D6 network, thereby providing a slowly decreasing voltage source.

F. VOLTAGE-TO-CURRENT CONVERTER CIRCUIT

With a voltage available which represents the laser drive current necessary to obtain the desired optical output (CLIP_SIG), a conversion circuit is necessary to actually produce the required supply current. Figure 4.16 serves as a general-purpose, low-power voltage-controlled current source. The sensitivity of the

voltage-to-current conversion is inversely proportional to the quality of R93; consequently, a precision-type resistor (in this case a 2% wire-wrapped device) is required for high accuracy.

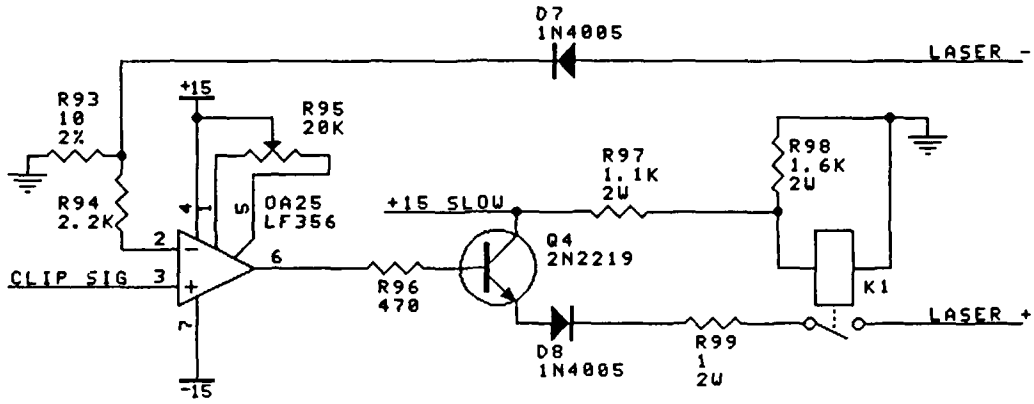

Figure 4.16. Voltage-Controlled Current Source (after Ref. 22).

The laser diode drive current I_{LD} is determined by

$$I_{LD} = \frac{\text{CLIP\_SIG}}{\text{R80}} \tag{4.6}$$

The voltage CLIP_SIG will typically vary between 0.35 V and 1.00 V (using the data available from Table 1), therefore the current supplied to the laser diode must necessarily range between 35 mA and 100 mA; currents which are much greater than 100 mA will possibly result in a catastrophic degradation of the laser diode's output and should therefore be limited by the circuit of Fig. 4.12. Since OA25 has a rated current of only 25 mA (verified by experimentation), a boosted output configuration for the current source is needed. Transistor Q4, rated at 100 mA with a 300 MHz bandwidth [Ref. 28:p. 4.93], is sourced from the "slow-

start" +15 V. Relay K1 is included to allow an even greater delay in the drive current during power-up and a quicker disconnect of current during power-down. Diodes D7 and D8 prevent potentially damaging reverse currents from reaching the laser diode. R99 facilitates the monitoring of the actual drive current; by placing a voltmeter across the 1 Ω resistor, the dc and ac components of the supply current can be measured.

As shown in Fig. 4.16, the laser anode will be connected to the point LASER_− and cathode to LASER_+. The current from OA19 will then modulate the forward-biased laser diode, which produces a current in the reverse-biased monitor photodiode and closes the power stabilization network loop.

G. SUMMARY

Although laser diodes have demonstrated extremely long lifetimes, their transfer functions (of changing electrical power into optical power) are greatly affected by age and operating environment. As devices get older or operate at changing temperatures, varying levels of drive current are required to produce the same level of optical power as new, temperature-stabilized diodes. In order to maintain a consistent performance throughout a laser diode's lifetime, the drive current must be continually monitored and (if necessary) modified to produce the desired optical power modulation. This stabilization network will compensate for most effects of gradual degradation and, with a signal clipping circuit, will help to reduce the likelihood of a catastrophic failure.

V. TEST AND EVALUATION

A. INTRODUCTION

Both stabilization networks--cooling and power--were subjected to several tests to evaluate their capabilities to drive a laser diode in steady-state conditions. By supplying various signal waveforms (sine/triangular/square waves at several frequencies) and by varying desired output parameters (device temperature, optical signal bias and modulation levels), the theoretical circuit design was evaluated regarding stability and dynamic range.

B. EVALUATION PROCEDURE

1. Test Equipment and Set-up

Figure 5.1 is a block diagram of the equipment used and the interconnections necessary in the system evaluation. A Wavetek Model 143 generates the modulated test signal to the power stabilization network. Both networks provide input to the Optologic TF-DIP Laser/LED test fixture which cradles the laser diode and provides a convenient method of obtaining feedback regarding module temperature and output power levels. Care *must* be taken to ensure the laser diode module's 14-pin DIP layout matches that of the Optologic fixture; different pin outlines might result in circuit damage or catastrophic failure of the module. The pigtail output of the laser diode is fed to a Photodyne Model 1600XP optical waveform analyzer which produces a voltage comparable to the

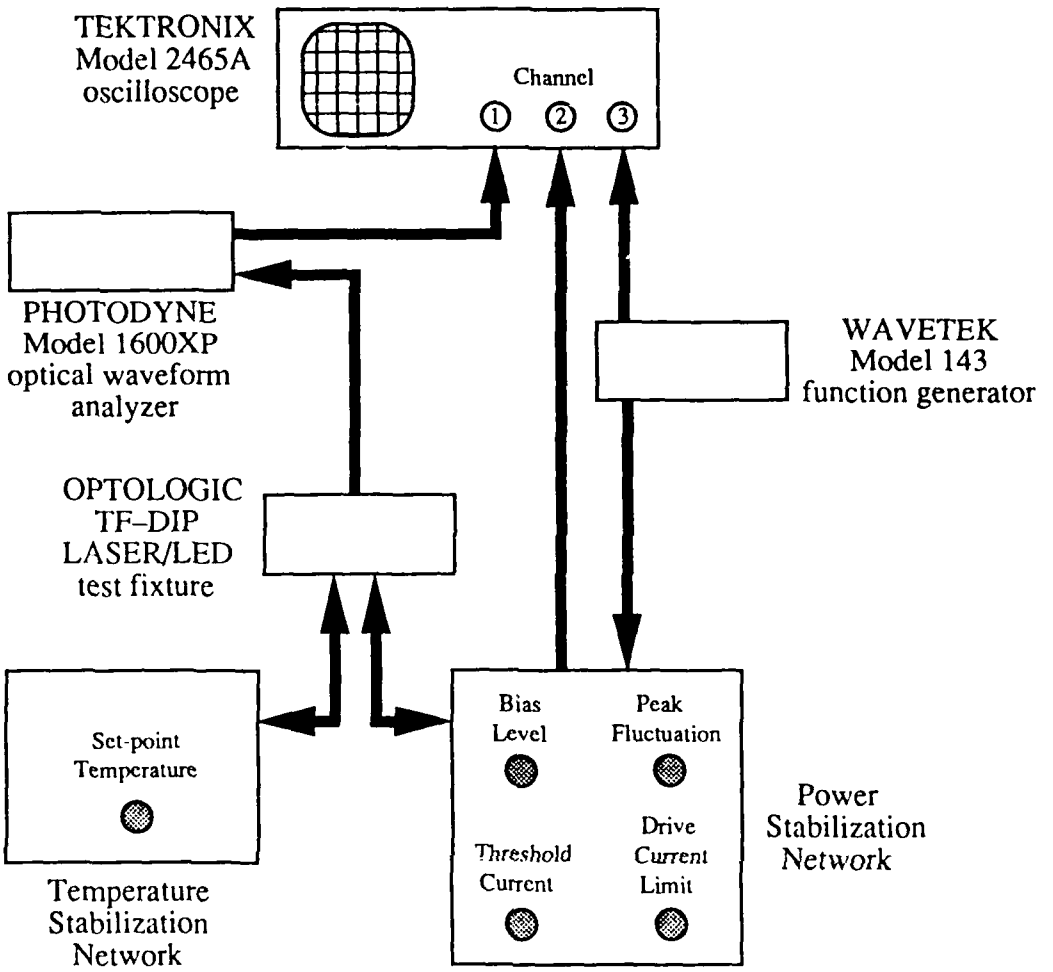

Figure 5.1. Test Equipment Set-up.

incident optical signal. This electrical signal, along with the monitor photodiode and original signal, are displayed on a Tektronix Model 2465A oscilloscope.

2. Operating Procedures

a. Start-up

To ensure safe operation of the laser module, this start-up procedure should be followed:

- Connect test equipment as shown in Fig. 5.1.
- Ensure that switch S1 is open (LED L1 should be off).
- Energize external power (±15 V dc and ±5 V/1 A dc sources).
- Adjust set-point temperature to desired operating point by setting the wiper voltage of R10 to the desired operating temperature accordirg to Eq. 3.10.
- Decrease the wiper voltage of R67 to set the threshold current as specified in the laser diode's data sheet; the wiper voltage varies between 0 and −1.0 V which corresponds to a threshold current range of 0 to 100 mA.
- Ensure that the wiper voltages of R52 (optical bias) and R71 (desired peak-to-peak optical fluctuation) are set to 0 V.
- Adjust R89 to set the necessary current limit level; the wiper voltage of R89 ranges between 0 and 5 V, corresponding to a current limit of 0 to 500 mA.
- Close S1 (L1 will light); after a few seconds, relay K1 will close allowing current to flow to the laser diode.
- Set the modulated signal amplitude fluctuation (via the Wavetek attenuation verniers) to the value corresponding to the desired optical power fluctuation (e.g., a 1.0 V peak-to-peak variance in input signal results in a 1.0 mW peak-to-peak fluctuation in the Lasertron module's output).
- Increase the wiper voltage of R52 to set the desired bias level; the wiper voltage varies between 0 and 1 V corresponding to a signal bias variation of 0 to 1.0 mW.
- Increase the wiper voltage of R71 to set the desired maximum variation in the modulated optical signal; the wiper voltage ranges between 0 and 0.1 V corresponding to a power fluctuation of 0 to 1.0 mW.

The reason that all power levels are initialized to zero *prior* to connecting the laser diode is one of device safety. With the laser diode disconnected, there is obviously no monitor photodiode signal entering the power stabilization network. If desired power levels were indeed specified at values greater than zero by R52, R67 or R71 prior to the connection of the laser diode

module, the integrator (OA13) would attempt to match its output to the *non-existent* monitor photodiode signal. Therefore, the output of the integrator could quickly saturate at several volts. Depending on the limiting value set by R89, this could lead to a bias current of several hundred milliamps being applied to the laser diode when S1 is closed and may result in a catastrophic degradation of the module. Consequently, desired operating levels are set *after* the laser diode module is connected to the network.

b. Laser Diode Modulation

The output waveforms on the oscilloscope should be closely monitored to ensure desired power levels are not exceeding the capability of the laser diode being tested. Temperature, signal bias and fluctuation levels can be varied to observe the effect on the optical waveform.

c. Shut-down

Whether powering-down of the networks is intentional or unintentional, the steps for a proper system shut-down are:

- Open S1 (L1 turns off).
- Reset the wiper voltages of R67 (threshold current), R52 (optical bias) and R71 (desired fluctuation) 0 V.
- Disconnect modulated test signal.
- Disconnect external power (±15 V dc and ±5 V/1 A dc sources).

C. DRIVING THE LASER DIODE WITH DC SIGNALS

1. Without Temperature Stabilization

Using only the power stabilization network, a dc drive current was applied to the laser diode in increasing levels from 0 to approximately 100 mA. Threshold current was set to −0.35 V (by R67) to correspond to the specification sheet threshold current of 35 mA, and the desired peak-to-peak fluctuation was set to 0 (at R71) to indicate a dc output is desired; no external signal was applied to the network (via OA17). Then by increasing the desired bias level (at R52), the unmodulated optical output can be changed. The drive current was monitored by the voltage drop across the 1 Ω resistor R99; an ammeter was used to display monitor photodiode current and thermistor resistance was read from an ohmmeter across the module's thermistor leads (since the cooling network was not connected). The actual optical output was converted by the Photodyne analyzer and displayed on the Tektronix oscilloscope. The Photodyne analyzer required approximately five minutes of warm-up time before readings could be taken; the analyzer produced an output of nearly −2.8 mV *without* an optical input, and the five minutes allowed the analyzer's output to stabilize at approximately 0 mV. Table 3 shows the results of this test. As can be expected, the trace on the oscilloscope was extremely "fuzzy" at lower output levels (less than 0.040 mW) since the laser diode is acting as an LED and not emitting coherent light with a narrow spectral width. As noted earlier, the increasing module temperature also affects the operation of the photodiode and small signals can be lost in such noise.

TABLE 3. RESPONSE WITHOUT TEMPERATURE STABILIZATION

Drive Current (mA)	Optical Output (mW)	Photodiode Current (mA)	Thermistor Resistance (kΩ)
3.6	0.0	0.0003	11.37
10.5	0.0	0.0005	11.05
15.0	0.0	0.0007	10.93
20.8	0.006	0.0011	10.71
25.0	0.010	0.0013	10.59
30.0	0.012	0.0017	10.39
35.0	0.016	0.0024	10.22
36.3	0.018	0.0028	10.16
37.0	0.022	0.0030	10.02
38.0	0.024	0.0040	9.99
39.0	0.040	0.0100	9.90
40.0	0.062	0.0186	9.86
41.0	0.084	0.0283	9.82
42.0	0.104	0.0384	9.78
43.0	0.128	0.0486	9.75
44.0	0.154	0.0601	9.69
45.0	0.178	0.0694	9.66
46.0	0.204	0.0777	9.60
47.0	0.226	0.0862	9.56
48.0	0.246	0.0968	9.53
49.0	0.270	0.1073	9.51
50.0	0.292	0.1169	9.42
51.0	0.320	0.1245	9.40
52.0	0.345	0.1333	9.37
53.0	0.365	0.1432	9.34
54.0	0.385	0.1526	9.30
55.0	0.410	0.1619	9.28
60.0	0.510	0.2045	9.15
65.0	0.610	0.2459	8.99
70.0	0.690	0.2815	8.76
75.0	0.780	0.3149	8.53
80.0	0.870	0.3450	8.36
85.0	0.930	0.3729	8.19

But once the drive current exceeded threshold, the optical power levels became very distinct. Figure 5.2 is a plot of the measured output power versus drive current; it has the classic form of a laser diode transfer function (see Fig. 2.2).

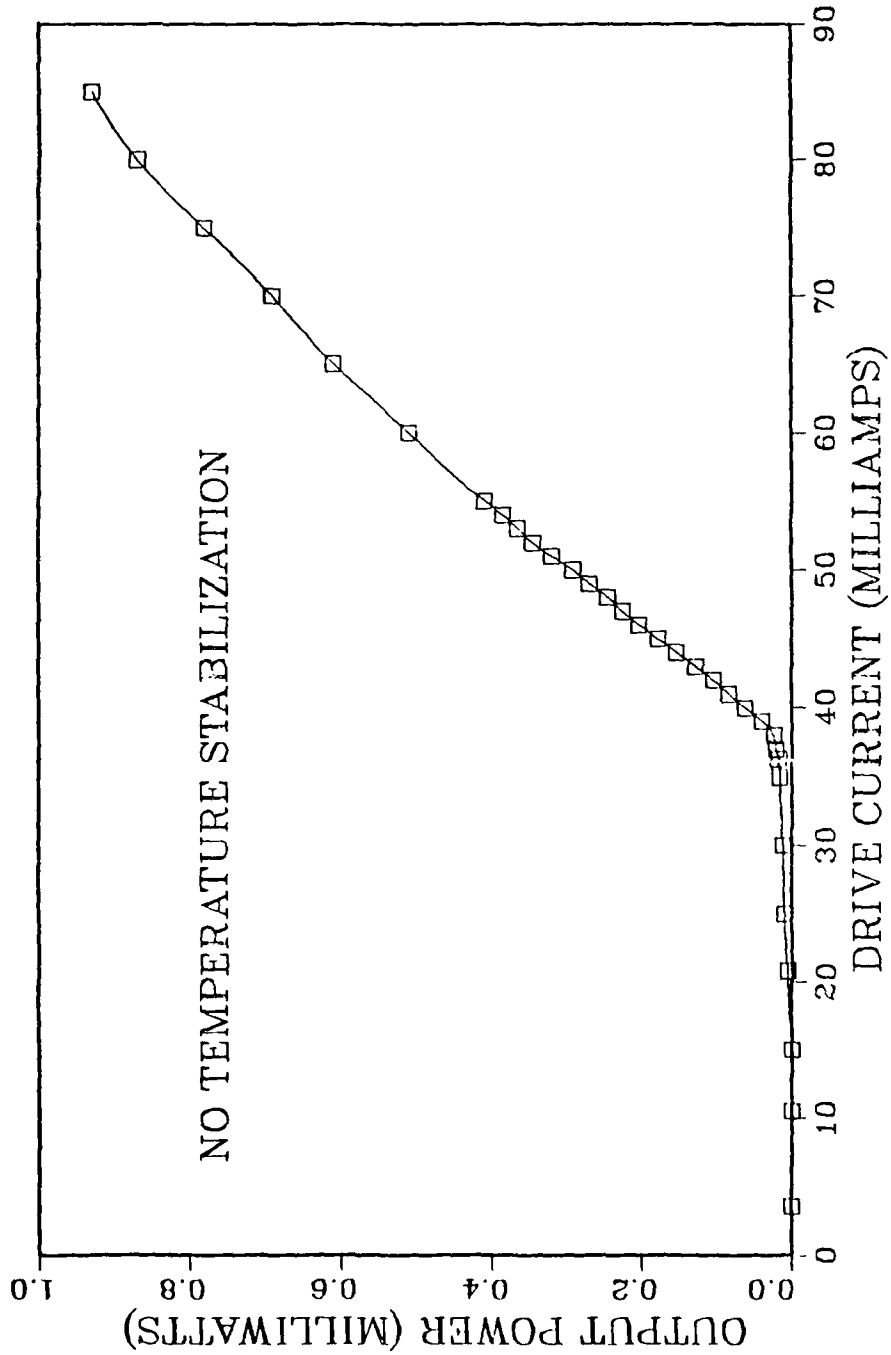

Figure 5.2. Optical Output versus Drive Current (Not Temperature Stabilized).

The measured photodiode activity is shown by the solid line in Fig. 5.3. Using linear regression and a least-squares fit, the data from Table 3 was modeled as

$$\text{Output Power} = 2.5\ \text{W-A}^{-1}(\text{Photodiode Current}) \tag{5.1}$$

In other words, the *measured* photodiode responsivity **R** is

$$\mathbf{R} = \frac{1}{2.5\ \text{W-A}^{-1}} = 0.4\ \text{A-W}^{-1} \tag{5.2}$$

This value is *four times* the specification sheet value (see Eq. 4.1). Consequently, in order to maintain the design criterion of a 1.0 V maximum output from OA4 (PD_OUT), R33 was changed from 10.0 kΩ to 2.5 kΩ; i.e.,

$$\text{PD\_OUT}_{max} = (I_{PD_{max}})(\text{R33}) \cong (0.4\ \text{mA})(2.5\ \text{k}\Omega) = 1.0\ \text{V} \tag{5.3}$$

This change preserves the basic assumptions behind the remainder to the power stabilization network.

Without temperature stabilization, it was expected that the thermistor resistance would decrease as the laser diode's output power increased. This was confirmed by the data in Table 3; Fig. 5.4 is a plot of the thermistor resistance versus output power. Using this data and Eq. 3.5, Fig. 5.5 was created which shows the relationship between module temperature and output power. It can be seen that the laser diode temperature quickly increased with little change in output and then gradually increased as the output increased. Consequently, this temperature variation affected the transfer function plotted in Fig. 5.2; this effect

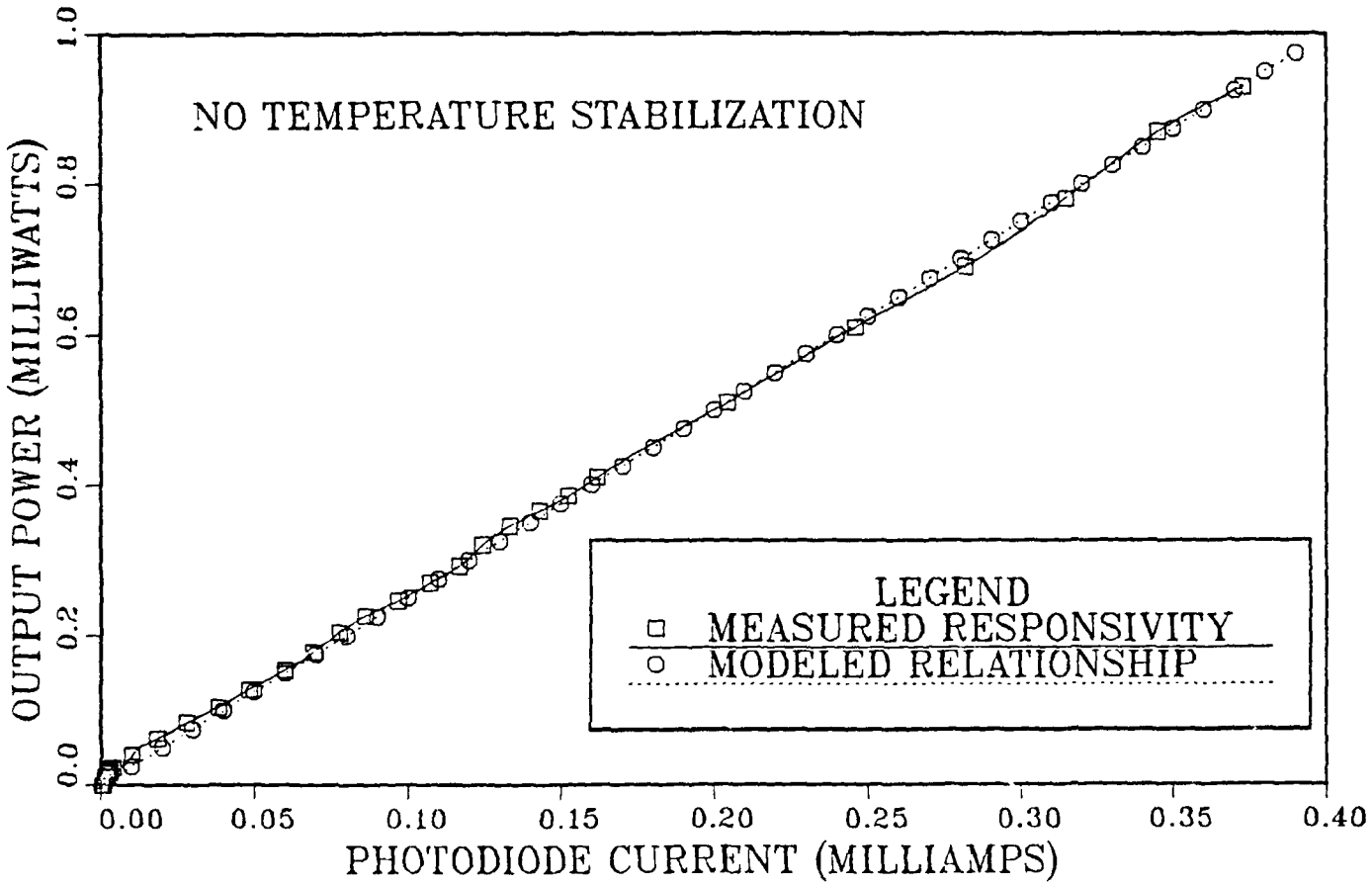

Figure 5.3. Optical Output versus Monitor Photodiode Current (Not Temperature Stabilized).

can be negated by connecting the temperature stabilization network designed in Chapter III.

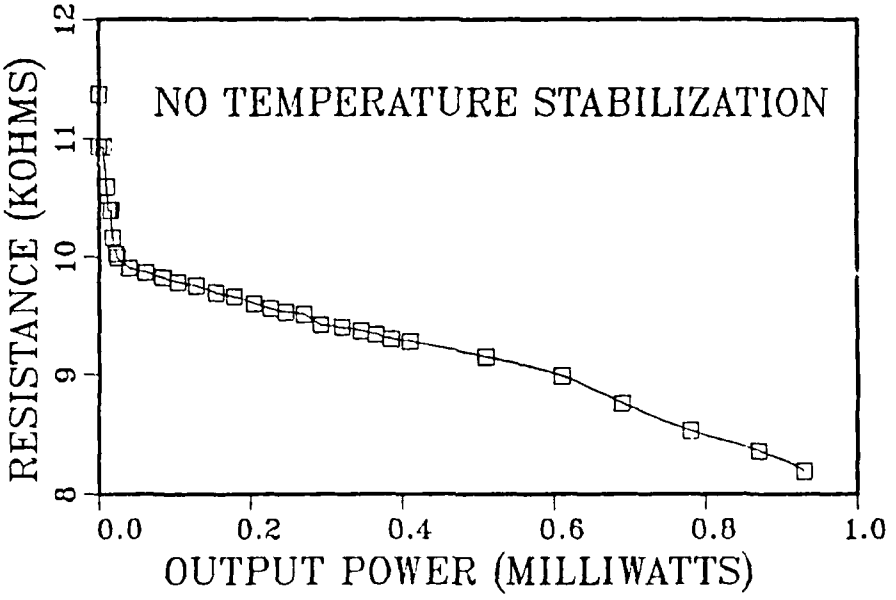

Figure 5.4. Thermistor Resistance versus Output Power.

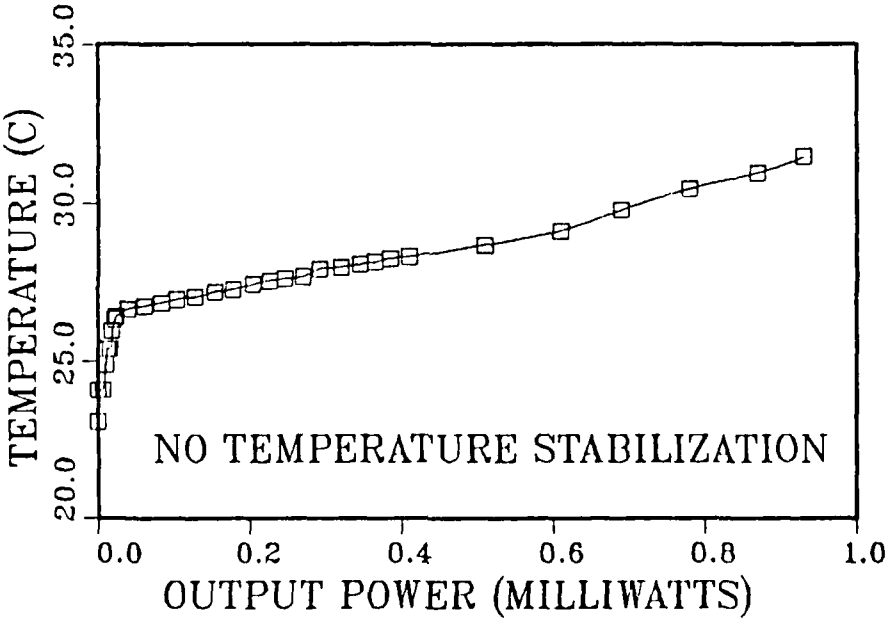

Figure 5.5. Module Temperature versus Output Power.

One final test was needed to compare the accuracy of the desired bias level to the actual optical output as measured on the oscilloscope. The wiper voltage of R52 was adjusted between 0.0 V and 0.9 V, representing a desired optical bias level of 0.0 mW to 0.9 mW. At the same time, the Photodyne analyzer output was monitored on the oscilloscope and on a digital voltmeter; with these devices, a 0.0 mV to 0.1 mV range represents a 0.0 mW to 1.0 mW laser diode output. The result of this test are shown in Table 4.

TABLE 4. DESIRED VERSUS ACTUAL OPTICAL OUTPUT BIAS LEVELS

Desired Optical Output (mW)	Actual Laser Diode Output (mW)
0.0	0.0
0.1	0.085
0.2	0.180
0.3	0.280
0.4	0.375
0.5	0.460
0.6	0.565
0.7	0.650
0.8	0.735
0.9	0.840

As can be seen, there is an offset of approximately −0.015 mW to −0.060 mW between desired and actual power levels; this difference can be explained by the approximation used in the transimpedance amplifier circuit and by the input offset voltages of the *unbalanced* op-amps used throughout the network [Refs. 24:p. 3.2 and 27:p. 136]. Although the offset is small and can be easily dealt with during operations, attempts were made to eliminate these differences. This could be

accomplished by altering summing ratios or op-amp biases somewhere within the whole network. However, changing resistor ratios in the network after the bias compensation circuit (Fig. 4.9) would also affect the peak-to-peak compensation values. Therefore, the problem would have to be dealt with solely by manipulating the elements in the bias compensation circuit. By altering the input resistances within the circuit, greater error was introduced. The only suitable results occurred when the offset voltage potentiometers in Fig 4.9 (R57, R64 and R70) were altered to reduce the difference between desired and actual output. Unfortunately, changing the offset nulls of the op-amps resulted in the saturation of the OA13 integrator at 4.5 V during power-up. This meant a surge of 450 mA through the laser diode when relay K1 was closed. To prevent such a dangerous situation, the op-amps of Fig. 4.9 were rebalanced by returning the nulling potentiometers to their original values. The differences noted in Table 4 would have to be taken into account during operation.

2. With Temperature Stabilization

The same test procedures were conducted on the laser diode as before, however the cooling network was activated and the module operating temperature was varied to determine its affect on optical output. The desired operating temperature was set by adjusting the wiper voltage of R10 according to Eq. 3.10. The current to the TEC was then allowed to stabilize *before* applying drive current. This brief period would allow the module to reach the desired operating temperature before output power began increasing (which increases the

temperature of the module as shown in Fig. 5.5). The wiper voltages and stable TEC currents used for the test are shown in Table 5.

TABLE 5. TEMPERATURE STABILIZATION TEST VALUES

Desired Operating Temperature (C)	R10 Wiper Voltage (V)	Stabilized TEC Current (mA)
15.0	1.2	98.1
20.0	1.4	26.3
25.0	1.6	−32.2
30.0	1.8	−32.2

The stabilized TEC current levels were necessary to offset the difference between set-point and ambient (22.5 C) temperatures. With a desired temperature *higher* than ambient, the TEC current was actually *heating* the module. This heating current peaked at −32.2 mA since this is the maximum value allowed from the −5 V/1 A source through R30 (see Fig. 3.6); this reverse-biased current was limited to this maximum to prevent damage to the TEC.

Table 6 shows the results from the drive currents applied to the laser diode stabilized at four different operating temperatures. Figure 5.6 displays this data plotted on a single graph; as discussed in Chapter II, an increase in set-point temperature from 15 C to 30 C results in an increase in threshold current from approximately 32.0 mA to 40.0 mA. There is however, little change in the slope of the lasing region of the four graphs.

The monitor photodiode current was also noted during the stabilization test to detect any dependence of responsivity to set-point temperature; Table 7 shows these results and Fig. 5.7 displays the data on one graph. The nearly

TABLE 6. TEMPERATURE-STABILIZED LASERTRON RESPONSE

Drive Current (mA)	Optical Output (mW) 15 C	20 C	25 C	30 C
0.0	0.0	0.0	0.0	0.0
9.0	0.016	0.006	0.0	0.008
15.0	0.024	0.016	0.0	0.014
20.0	0.030	0.020	0.0	0.020
25.0	0.036	0.026	0.004	0.022
30.0	0.038	0.030	0.009	0.026
35.0	0.076	0.032	0.013	0.028
36.0	0.100	0.038	0.016	0.028
37.0	0.122	0.064	0.018	0.030
38.0	0.148	0.092	0.022	0.032
39.0	0.174	0.116	0.035	0.034
40.0	0.202	0.140	0.060	0.034
41.0	0.226	0.166	0.086	0.038
42.0	0.250	0.190	0.110	0.048
43.0	0.274	0.212	0.136	0.070
44.0	0.300	0.238	0.162	0.092
45.0	0.330	0.260	0.188	0.122
46.0	0.350	0.284	0.210	0.148
47.0	0.375	0.312	0.236	0.172
48.0	0.400	0.340	0.260	0.192
49.0	0.425	0.365	0.285	0.216
50.0	0.440	0.385	0.310	0.240
55.0	0.555	0.510	0.425	0.365
60.0	0.680	0.625	0.540	0.475
65.0	0.760	0.710	0.640	0.580
70.0	0.870	0.830	0.740	0.680
75.0	0.950	0.900	0.820	0.770
80.0	1.000	0.990	0.910	0.860
85.0	1.000	1.020	0.990	0.940

coincident lines indicate the monitor photodiode's responsivity is nearly constant over "normal" operating temperature ranges. This simplifies the total network design by alleviating the need to compensate the photodiode output current for temperature differentials.

TABLE 7. TEMPERATURE DEPENDENCE OF PHOTODIODE CURRENT

Photodiode Current (mA)/Optical Output (mW)

15 C	20 C	25 C	30 C
0.0002/0	0.0003/0	0.0002/0	0.0002/0
0.0005/0.016	0.0005/0.006	0.0005/0	0.0005/0.008
0.0009/0.024	0.0008/0.016	0.0007/0	0.0008/0.014
0.0012/0.030	0.0011/0.020	0.0011/0	0.0010/0.020
0.0016/0.036	0.0014/0.026	0.0014/0.004	0.0013/0.022
0.0022/0.038	0.0019/0.030	0.0017/0.009	0.0016/0.026
0.0188/0.076	0.0034/0.032	0.0024/0.013	0.0021/0.028
0.0306/0.100	0.0053/0.038	0.0026/0.016	0.0022/0.028
0.0421/0.122	0.0167/0.064	0.0031/0.018	0.0024/0.030
0.0544/0.148	0.0282/0.092	0.0039/0.022	0.0026/0.032
0.0661/0.174	0.0393/0.116	0.0097/0.035	0.0028/0.034
0.0769/0.202	0.0504/0.140	0.0203/0.060	0.0032/0.034
0.0890/0.226	0.0616/0.166	0.0307/0.086	0.0040/0.038
0.1005/0.250	0.0718/0.190	0.0420/0.110	0.0082/0.048
0.1112/0.274	0.0825/0.212	0.0528/0.136	0.0175/0.070
0.1220/0.300	0.0937/0.238	0.0628/0.162	0.0273/0.092
0.1336/0.330	0.1045/0.260	0.0724/0.188	0.0380/0.122
0.1440/0.350	0.1150/0.284	0.0825/0.210	0.0481/0.148
0.1548/0.375	0.1260/0.312	0.0924/0.236	0.0588/0.172
0.1661/0.400	0.1378/0.340	0.1031/0.260	0.0686/0.192
0.1781/0.425	0.1480/0.365	0.1132/0.285	0.0787/0.216
0.1887/0.440	0.1586/0.385	0.1242/0.310	0.0877/0.240
0.2425/0.555	0.2101/0.510	0.1747/0.425	0.1352/0.365
0.2939/0.680	0.2608/0.625	0.2223/0.540	0.1811/0.475
0.3459/0.760	0.3084/0.710	0.2685/0.640	0.2238/0.580
0.3901/0.870	0.3515/0.830	0.3097/0.740	0.2651/0.680
0.4369/0.950	0.3968/0.900	0.3522/0.820	0.3023/0.770
0.4520/1.000	0.4338/0.990	0.3880/0.910	0.3391/0.860
	0.4518/1.020	0.4248/0.990	0.3705/0.940

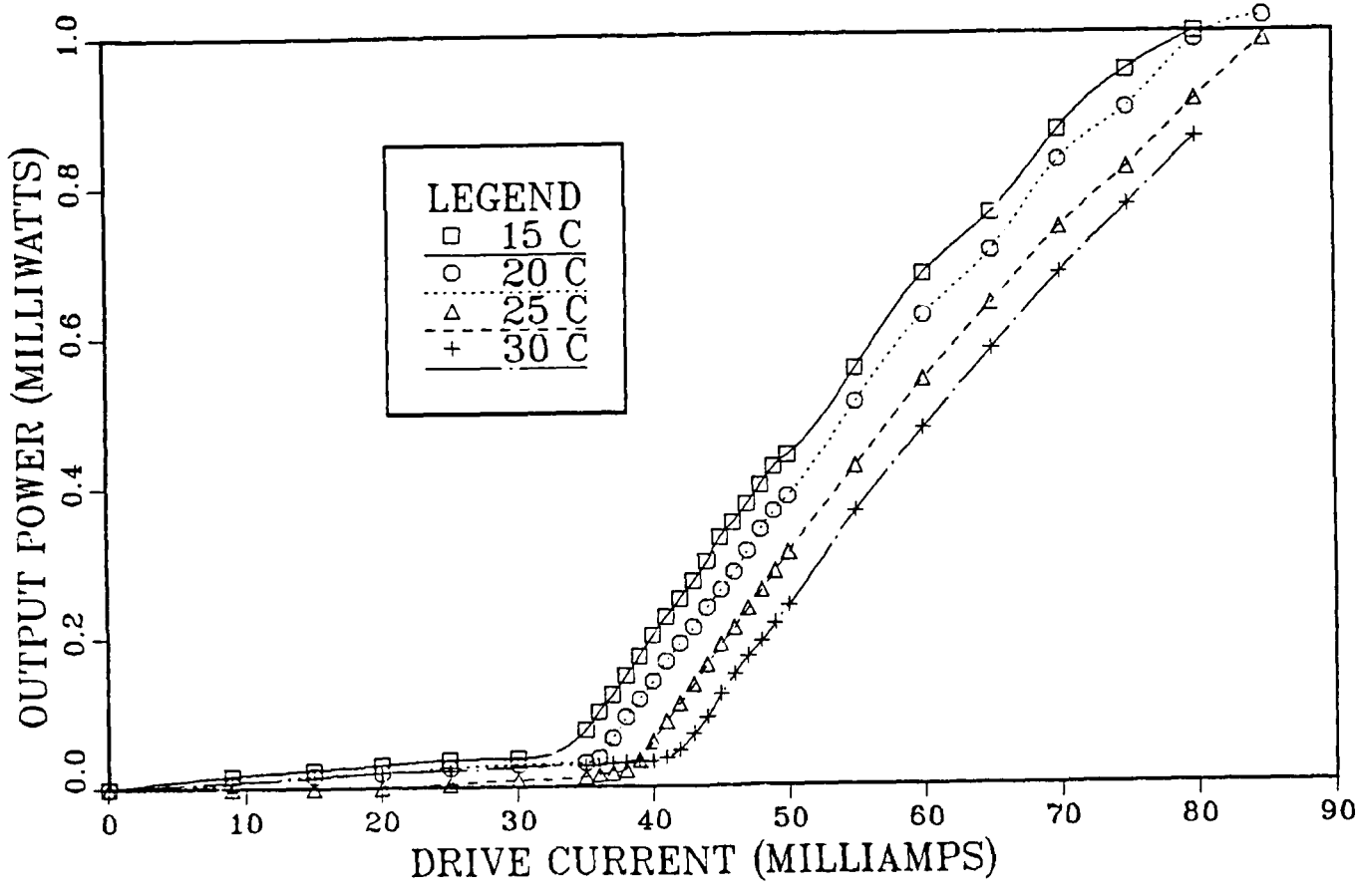

Figure 5.6. Optical Output versus Drive Current (Temperature Stabilized).

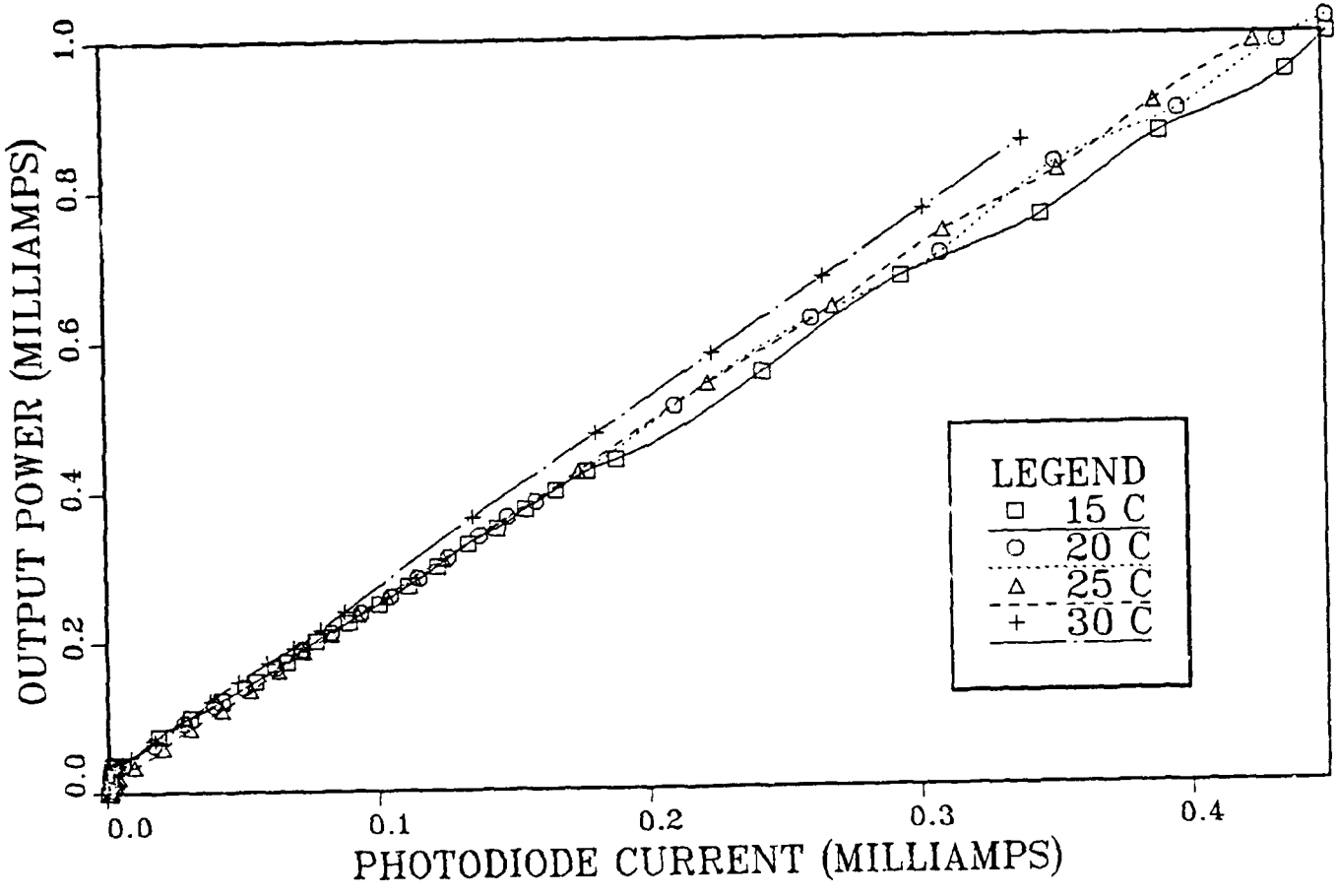

Figure 5.7. Optical Output versus Monitor Photodiode Current (Temperature Stabilized).

D. MODULATING THE LASER DIODE

1. Verifying Network Design

An external modulation signal was connected to the stabilization networks (both power and temperature) and the laser diode was tested with various waveforms of different frequencies. Figure 5.8 is a typical optical waveform as transformed the Photodyne analyzer into an electrical signal; with a desired bias level of 0.5 mW at a frequency of 100 kHz, a sine wave was sent through the laser diode producing a 50.0 mV biased, 100 kHz modulated signal.

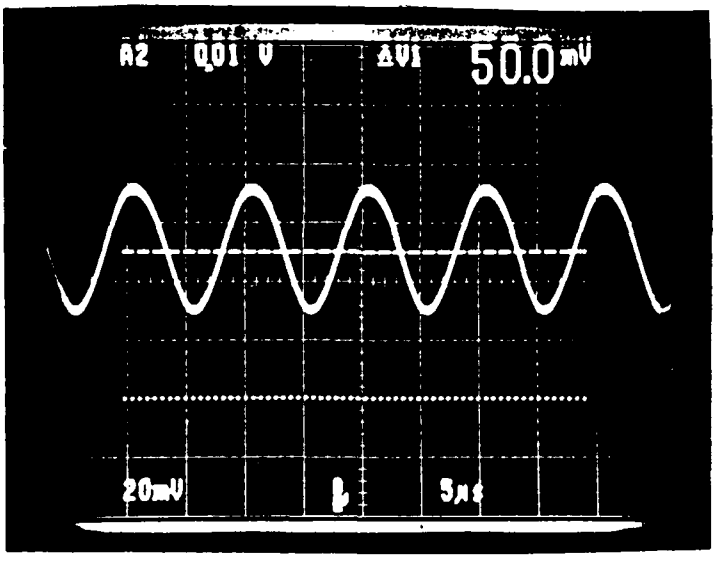

Figure 5.8. Modulated Laser Diode Output.

As was done with the dc bias level adjustment, a test was conducted to verify the correlation between desired peak-to-peak fluctuation (as set by R71 in Fig. 4.10) with the actual output observed on the oscilloscope. The waveform of Fig 5.8 was used in this experiment; with the desired bias level set at 0.5 mW,

the frequency kept at 100 kHz and the temperature stabilized to 25 C, the input signal amplitude was varied (using the Wavetek). The desired fluctuation level was set via the wiper voltage of R71; the variation of 0 to 100 mV corresponded to a 0 to 1 mW peak-to-peak power fluctuation. It was quickly seen that the optical output from the stabilization network was greater than the desired fluctuation by a factor of two; therefore, R85 (Fig. 4.11) was changed from 2.0 kΩ to 4.22 kΩ to correct the problem. Table 8 shows the comparisons of desired to realized power fluctuation obtained in this experiment *before* and *after* changing R85.

TABLE 8. DESIRED VERSUS ACTUAL OUTPUT POWER FLUCTUATION

	Actual Output Fluctuation (mW)	
Desired Fluctuation (mW)	R85 = 2.0 kΩ	R85 = 4.22 kΩ
0.05	0.100	0.052
0.10	0.215	0.106
0.15	0.320	0.190
0.20	0.420	0.218
0.25	0.540	0.262
0.30		0.322
0.40		0.426
0.50		0.535
0.60		0.625
0.70		0.735
0.80		0.810
0.90		0.900

The remaining error in results can be attributed to the approximation used in the transimpedance amplifier circuit.

It should be noted that measurements were difficult to make at the extremes of the optical output; the low power levels (less than 0.190 mW) produced traces on the oscilloscope which were extremely "fuzzy" while the higher power levels (above 0.8 mW) resulted in waveforms with jitter. This "fuzziness" may be due to the fact that the dc bias applied to the laser diode was not large enough to produce a sharp output; experiments have shown that drive currents at or near threshold can show significant output distortion while small increases in the bias current greatly improve the "cleanliness" of the optical output [Ref. 29:p. 247]. The solution to this problem may seem obvious: increase the dc bias. Unfortunately, this technique results in the second noted distortion, that of jitter. Laser diodes tend to exhibit such stationary self-pulses (i.e., jitter) when they are dc biased to values over a few percent above threshold; this behavior may become more apparent as the module ages, although the rate of the pulsations (normally 0.1 to a few GHz) may decrease with time [Refs. 30:p. 231 and 31:p. 565].

With R85 changed to 4.22 kΩ, Figs. 5.9 and 5.10 were taken to confirm the network's peak-to-peak stabilization capability. The desired peak-to-peak fluctuation in both cases (and in Fig 5.8) was 0.4 mW, with the actual results are shown in the figures (a cursor ΔV value of 40.0 mV equates to a peak-to-peak power fluctuation of 0.4 mW). The actual fluctuation is close to the desired level and differences can be attributed to the transimpedance amplifier resistor ratios (as mentioned earlier) and oscilloscope reading approximations.

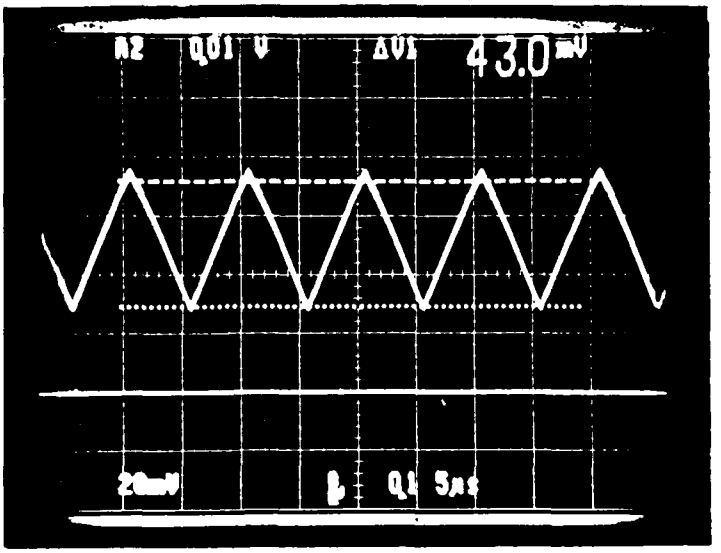

Figure 5.9. Modulated Triangular Wave.

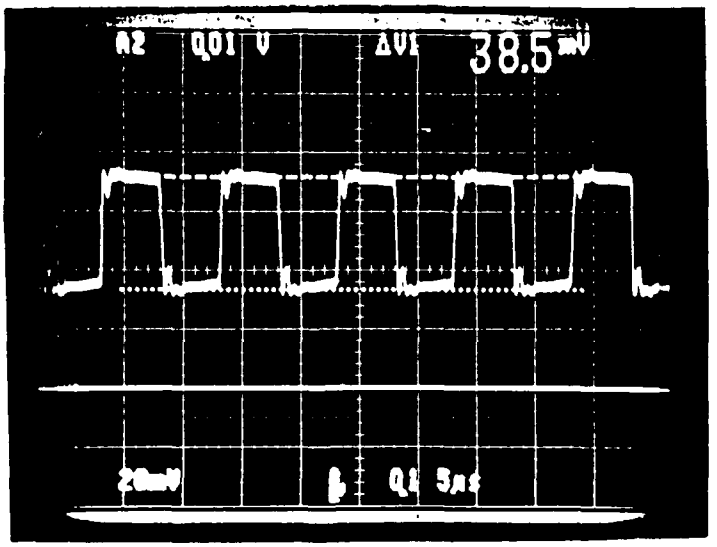

Figure 5.10. Modulated Square Wave.

As a final check of the limiting circuit (Fig. 4.12), the maximum drive current was reduced to 60 mA by reducing the wiper voltage of R89 to 0.6 V. The same sinusoid of Fig. 5.8 was then sent through the network and the resulting waveform is shown in Fig. 5.11. The desired peak-to-peak fluctuation remains at

0.4 mW (represented by the oscilloscope ΔV of 40.5 mV); however the waveform is clipped at 0.6 mW (at the 60 mV graticule). There is an overshoot which lasts for 1.3 s and exceeds the desired power clipping level by approximately 0.12 mW (i.e., 12.0 mV on the oscilloscope trace). This problem can be attributed to the typical 1.5 s settling time of the LF356 and the nominal 10% overshoot expected from each EL2041 [Refs. 24:p. 3.2 and 27:p. 1.137].

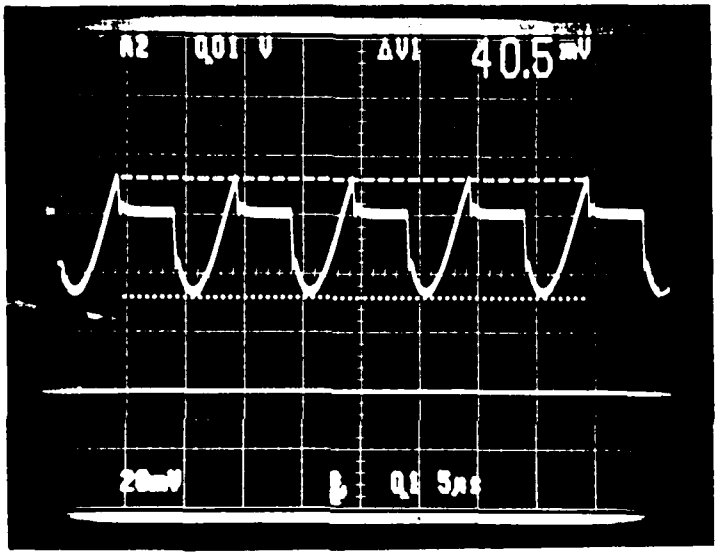

Figure 5.11. Current-limited Waveform.

2. Too Little/Too Much Output Bias

Figure 5.12 demonstrates the effect of *too little* optical bias and too much signal modulation. With the bias level set at 0.15 mW (i.e., 15.0 mV on the oscilloscope), a signal with *over* 0.34 mW of desired optical modulation was transmitted through the laser. As can be seen, the laser actually shuts off during part of the transmission cycle. Although this technique may be useful for an "on-

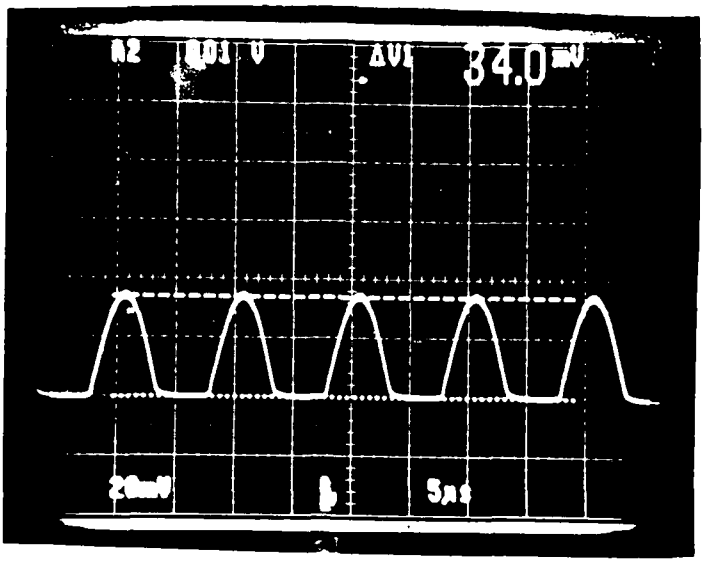

Figure 5.12. Modulation With Too Little Bias.

off keying" (OOK) communication scheme, the driving of the laser diode below threshold greatly reduces the speed at which an electrical signal can be converted into optical power.

On the other hand, Fig. 5.13 is the result of a modulated signal with *too much* optical bias. The output of the laser diode clearly shows distortion as the optical power approaches (or tries to exceed) the maximum rating of the laser diode. Distortion in the upper peaks of the sine wave indicates the attempt at "overdrive," and this may result in damage to the laser diode if continued. As mentioned previously in Chapter IV, care must be taken *not* to underdrive or overdrive the laser diode module; desired bias and fluctuation levels need to be compared so that the optical output does not produce unexpected (as in Fig 5.12) or potentially dangerous (as in Fig 5.13) results for the laser diode.

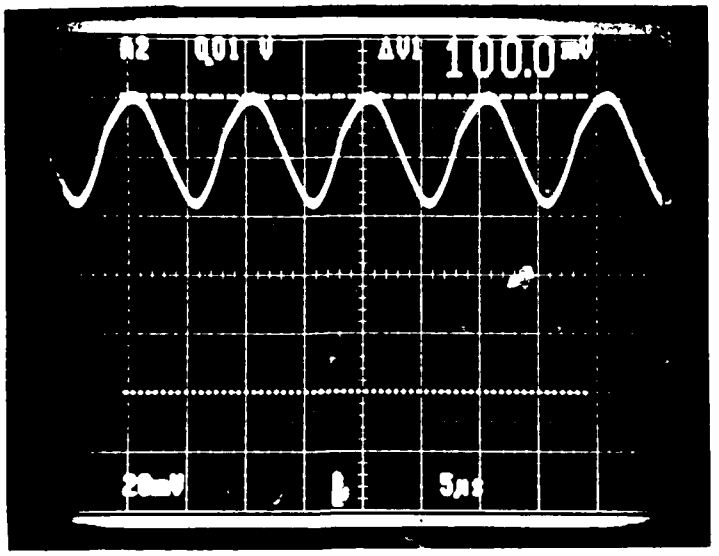

Figure 5.13. Modulation With Too Much Bias.

3. Minimum/Maximum Modulation Limits

The power stabilization network was then adjusted to determine the minimum and maximum limits of modulation. After setting the desired optical bias level to a convenient median value (in the next two cases, 0.5 mW), the desired peak-to-peak fluctuation level (at R71) and the input signal (into OA17) were varied to find the smallest and largest signal which could be identified on the oscilloscope trace. Figure 5.14 shows the result of a desired fluctuation of 0.004 mW being set at R71 (with a wiper voltage of 0.4 mV) and an input signal of 4.0 mV peak-to-peak amplitude being applied. Despite the quality of the oscilloscope trace, the resulting optical output can be distinguished as a sinusoidal with a power fluctuation of approximately 0.021 mW. This can be considered the *minimum* signal fluctuation which can be transmitted by this network (and test

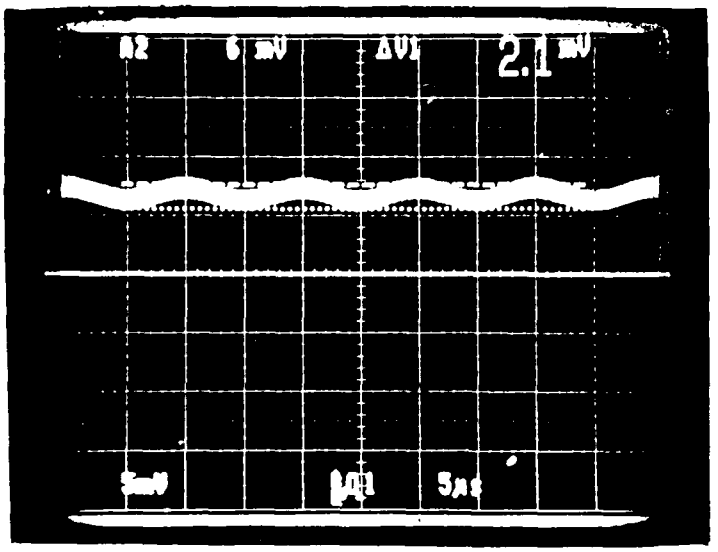

Figure 5.14. Minimum Detectable Modulation.

equipment); the difference between desired and realized signal values are for the same reasons discussed previously. Similarly, Fig. 5.15 shows the *maximum* signal

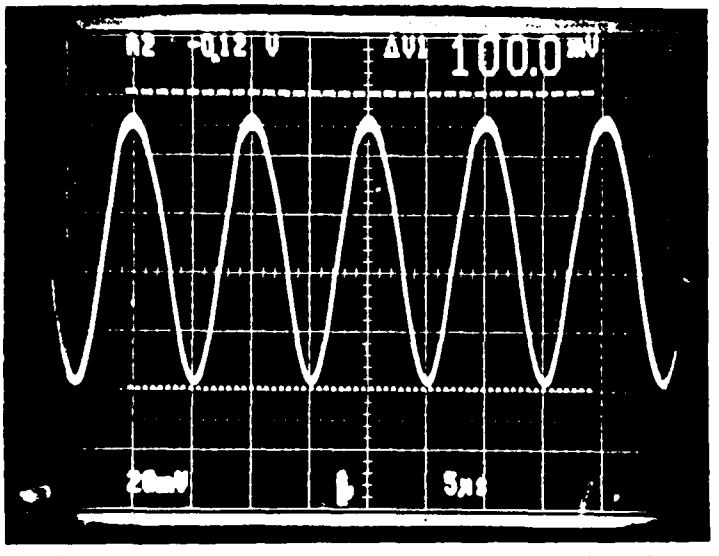

Figure 5.15. Maximum Allowable Modulation.

fluctuation allowed. The desired peak-to-peak variance was set to 0.9 mW by adjusting a 90.0 mV wiper voltage at R71 (the largest value allowable by design). The input signal was also changed to a 0.9 V peak-to-peak amplitude and the high optical power peaks are beginning to demonstrate the distortion shown previously. Figures 5.14 and 5.15 show the wide range of possible signal levels which can be handled by these stabilization networks.

4. Dynamic Range

Although most of the design work for these networks has used test signals with frequencies at or near 100 kHz, an examination of the system's performance with signal frequencies over a wide spectrum is necessary. To observe these reactions, two pieces of equipment were added to the test set-up of Fig. 5.1. The signal from the Wavetek function generator was also applied to an HP 5328A frequency counter in order to obtain an accurate frequency measurement. In addition, an HP 3575A gain-phase meter was connected in order to determine the amplitude and phase changes between the actual optical waveform (from the Photodyne analyzer) and a reference signal (from the same Wavetek generator producing the actual input signal).

The signal amplitude noted at 100 kHz was used as a reference for all measurements. Since an input modulation variation of 0.5 V produced an output from the Photodyne analyzer of 50.0 mV (an input fluctuation of 0.5 V indicates a desired optical output change of 0.5 mW which translates to a Photodyne output of 50.0 mV), there is an *expected* amplitude difference between the reference

signal and actual output at 100 kHz. Therefore all the gain measurements taken from the HP 3575A were offset by the necessary correction factor; i.e.,

$$\text{Correction Factor} = 20 \log\left[\frac{40 \text{ mV}}{0.4 \text{ V}}\right] = -20 \text{ dB} \tag{5.4}$$

With the operating temperature stabilized to 25 C, an optical bias of 0.5 mW and a desired peak-to-peak fluctuation set at 0.4 mW (similar to Fig. 5.1), the input signal's frequency was changed and data taken. Table 9 shows the results of this experiment.

TABLE 9. GAIN-PHASE RESPONSE OF STABILIZATION NETWORK

Frequency (kHz)	Amplitude (dB)	Phase (degrees)
0.5	−12.5	−140.0
1.0	−9.2	86.0
2.0	−4.5	60.6
5.0	−2.7	33.7
10.0	−2.1	19.3
15.0	−1.7	11.5
20.0	−1.4	7.2
50.0	−0.3	2.7
100.0	0.0	−7.2
150.0	0.4	−19.3
200.0	0.9	−29.1
500.0	1.7	−81.6
1000.0	1.8	−164.9
1500.0	0.6	84.6
2000.0	−3.7	−17.5
3000.0	−9.7	−163.0
4000.0	−13.0	84.6
5000.0	−10.8	24.5

Severe distortion occurred in the sinusoidal output at frequencies below 5.0 kHz and above 5.0 MHz; therefore data in these regions was not taken. A negative

phase value in Table 9 indicates the output waveform lags the reference signal; a positive phase means the output lags the reference by 180 degrees *plus* the value shown (i.e., a phase difference of 86.0 degrees means the output lags the reference by 266.0 degrees).

Figure 5.16 is a Bode plot of the data from Table 9. The figure indicates the stabilization network has a reasonable response between 2.0 kHz and 2.0 MHz, with system losses less than 5.0 dB. Performance at lower frequencies can be improved by substituting slower, but higher precision op-amps (such as the OP-07 family). Higher frequency response would require faster, larger bandwidth integrated circuits or a complete network redesign using matched, discrete components.

E. SUMMARY

The tests used in this chapter adequately evaluated the performance of the temperature and power stabilization networks. Data obtained from the tests verified the validity of the designs and proved that the circuits satisfied the basic system criteria established in Chapter I. Some capabilities exceed those initially required and demonstrate the flexibility of the networks.

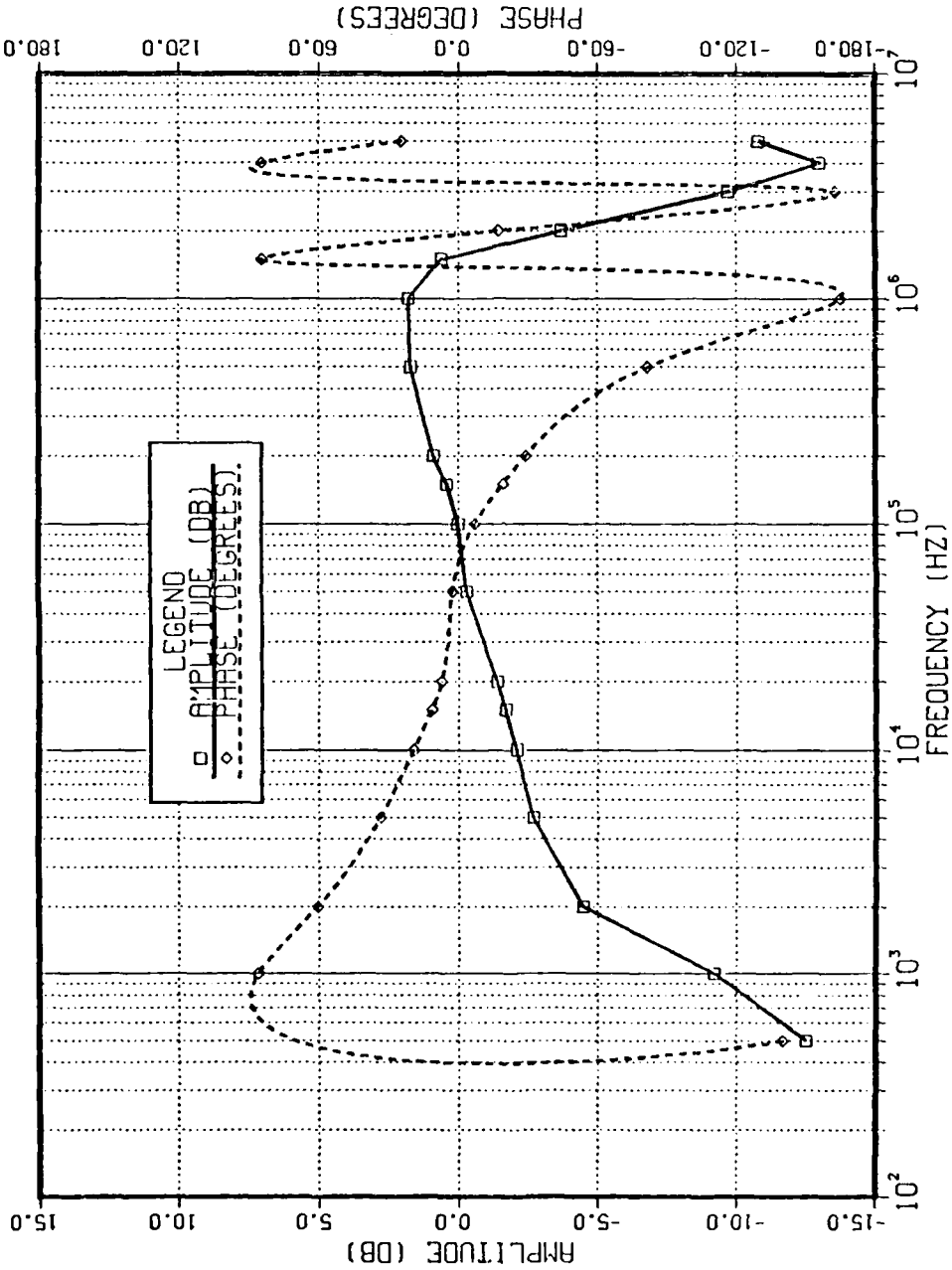

Figure 5.16. Dynamic Range of Stabilization Networks.

VI. CONCLUSIONS

A. SUMMARY OF RESULTS

This thesis accomplished the major objectives as outlined in Chapter I. The circuit development has included a great deal of flexibility which allows the driving of a wide array of light-producing devices using low-voltage power sources. By simply changing certain resistors, laser diode modules with different responsivities and power transfer functions can be accommodated. Network testing has demonstrated the system's ability to modulate a laser diode at rates between 2.0 kHz and 2.0 MHz without appreciable loss (less than 5.0 dB); stable outputs were noted within this range of frequencies for various input levels. Module protection against supply surges was provided by power delay circuits, and overall drive currents were adequately limited by a signal clipping network. Finally, the capability of the temperature stabilization network was readily apparent by its effect on the optical output of the laser diode during testing; its cooling abilities were limited only by the characteristics of the TEC mounted inside the laser diode module and by the output of the high-current power sources.

B. AREAS FOR FURTHER STUDY

To properly test the stabilization networks, the effects of long-term operation need to be considered; therefore, experiments of several hours (if not days) of continuous modulation must be conducted. By monitoring voltages and currents

at key points, the capability of the design can be truly assessed. Utilizing the networks in extreme environments can also be explored; underwater, desert or arctic communications are three possible applications. Such remote operations would also benefit from the construction of smaller, higher-power voltage sources.

Methods to improve the dynamic range of the system may be investigated by replacing components with devices of higher bandwidths; however this may require some redesign to eliminate the need for complex (and relatively slow) integrated circuits such as the AD534 and AD834 multipliers.

The drive system can be expanded to become the center of a total communication scheme which uses a wide variety of analog encoding. This would also include the design and implementation of a receiver network as well as encoding/decoding hardware. In addition, a slight modification to the bias compensation circuit would allow the design to process digital vice analog modulation schemes.

LIST OF REFERENCES

1. R.W. Campbell and F.M. Mims III, *Semiconductor Diode Lasers*, Howard W. Sams, Co., Indianapolis, Indiana, 1972

2. J.M. Senior, *Optical Fiber Communications: Principles and Practice*, Prentice-Hall, Englewood Hills, New Jersey, 1985

3. H. Kressel, M. Ettenberg, J.P. Wittke and I. Ladany, "Laser Diodes and LEDs for Fiber Optical Communication," in *Topics in Applied Physics: Semiconductor Devices for Optical Communication, Vol. 39, 2d. ed.*, H. Kressel, ed., pp. 9-60, Springer-Verlag, New York, 1982

4. F.K. Reinhart, K. Hayashi and M.B. Panish, "Mode Reflectivity and Waveguide Properties of Double-Heterostructure Injection Lasers," in *Semiconductor Injection Lasers*, J.K. Butler, ed., pp. 92-105, IEEE Press, New York, 1980

5. E. Pinkas, B.I. Miller, I. Hayashi and P.W. Foy, "GaAs-$Al_xGa_{1-x}As$ Double Heterostructure Lasers: Effect of Doping on Lasing Characteristics of GaAs," in *Semiconductor Injection Lasers*, J.K. Butler, ed., pp. 234-242, IEEE Press, New York, 1980

6. Notes for EC3550 (Fiber Optic Systems Fundamentals), Naval Postgraduate School, 1989 (unpublished)

7. J.C. Palais, *Fiber Optic Communications*, 2d. ed., Prentice-Hall, Englewood Cliffs, New Jersey, 1988

8. J.P. Powers, *EC 3210 Notes*, Naval Postgraduate School, Monterey, California, 1989 (unpublished)

9. M. Ettenberg and D. Sarnoff, "Specifications and Characteristics of Laser Diodes for the User," in *Optical Component Specifications for Laser-Based Systems and Other Modern Optical Systems, SPIE Critical Review of Technology Series, Vol. 607*, R.E. Fisher and W.J. Smith, eds., pp. 161-167, International Society for Optical Engineering, Bellingham, Washington, 1986

10. H. Kressel and M. Ettenberg, "Light Sources--An Update," in *Topics in Applied Physics: Semiconductor Devices for Optical Communication, Vol. 39,*, 2d. ed., H. Kressel, ed., pp. 285-291, Springer-Verlag, New York, 1982

11. P.K. Cheo, *Fiber Optics: Devices and Systems*, Prentice-Hall, Englewood Cliffs, New Jersey, 1985

12. D.G. Baker, *Monomode Fiber-Optic Design: With Local-Area and Long-Haul Network Applications*, Van Nostrand Reinhold Company, New York, 1987

13. *Optics Guide 3*, Melles Griot, Irvine, California, 1985

14. R.G. Hunsperger, *Integrated Optics: Theory and Technology*, Springer-Verlag, New York, 1982

15. H. Kressel and H.F. Lockwood, "A Review of Gradual Degradation Phenomena in Electroluminescent Diodes," in *Semiconductor Injection Lasers*, J.K. Butler, ed., pp. 290-298, IEEE Press, New York, 1980

16. S.A. Esty, "Transmitting Video by Light," *Installer/Technician*, December 1988, reprint from Corning Incorporated, Corning, New York, 1990

17. Specification Sheet for LASERTRON GaInAsP/InP QLM-1300-SM-BH laser module, part number QLM-1300SM-101, serial number 5020583, Burlington, Massachusetts, 1985

18. Application Notes for Thermoelectric Devices, Materials Electronic Products Corporation, Trenton, New Jersey, 1987

19. L.A. Johnson, "Controlling Temperatures of Diode Lasers and Detectors Thermoelectrically," *Lasers & Optronics*, pp. 109-114, April 1988

20. "Linear Circuits: Voltage Regulators and Supervisors," Texas Instruments Inc., Dallas, Texas, 1989

21. *SDL-800 Laser Diode Driver User's Manual*, Spectra Diode Labs, San Jose, California, November 1986

22. W.G. Jung, *IC Op-Amp Cookbook*, 3d. ed., Howard W. Sams & Co., Indianapolis, Indiana, 1988

23. J.P. Powers, *An Introduction to Fiber Optic Systems*, Naval Postgraduate School, Monterey, California, 1987 (unpublished)

24. "Linear Databook," National Semiconductor Corporation, Santa Clara, California, 1980

25. "Linear Products Databook," Analog Devices, Inc., Norwood, Massachusetts, April 1988

26. "Integrated Circuits," Analog Devices, Inc., Norwood, Massachusetts, April 1984

27. "1990 Data Book: Monolithic & Hybrid Integrated Circuits," Élantec, Inc., Milpitas, California, 1988

28. "The Transistor and Diode Data Book for Design Engineers," Texas Instruments Incorporated, Dallas, Texas, 1973

29. C.L. Tang, ed., *Quantum Electronics: Methods of Experimental Physics, Volume 15, Part A*, Academic Press, New York, 1979

30. G. Arnold, P. Russer and K. Petermann, "Modulation of Laser Diodes," in *Topics in Applied Physics: Semiconductor Devices for Optical Communication, Volume 39*, 2d. ed., H. Kressel, ed., pp. 213-242, Springer-Verlag, New York, 1982

31. I.V. Kaminow and T. Li, "Modulation Techniques," in *Introduction to Optical Fiber Communications*, Y. Suematsu and K. Iga, eds., pp. 557-593, John Wiley & Sons, Inc., New York, 1982

INITIAL DISTRIBUTION LIST

		No. of Copies
1.	Defense Technical Information Center Cameron Station Alexandria, Virginia 22304-6145	2
2.	Library, Code 52 Naval Postgraduate School Monterey, California 93943-5002	2
3.	Department Chairman, Code EC Department of Electrical and Computer Engineering Naval Postgraduate School Monterey, California 93943-5002	1
4.	Professor John P. Powers, Code EC/Po Department of Electrical and Computer Engineering Naval Postgraduate School Monterey, California 93943-5002	4
5.	Professor Sherif Michael, Code EC/Mi Department of Electrical and Computer Engineering Naval Postgraduate School Monterey, California 93943-5002	2
6.	Commandant of the Marine Corps Code TE 06 Headquarters, U.S. Marine Corps Washington, D.C. 20380-0001	1